

## Structure-Affinity Relationship Studies on 5-HT<sub>1A</sub> Receptor Ligands. 2. Heterobicyclic Phenylpiperazines with N4-Aralkyl Substituents

Bart J. van Steen,<sup>\*,†</sup> Ineke van Wijngaarden,<sup>†</sup> Martin Th. M. Tulp,<sup>‡</sup> and Willem Soudijn<sup>§</sup>

Departments of Medicinal Chemistry and Pharmacology, Solvay Duphar Research Laboratories, P.O. Box 900, 1380 DA Weesp, The Netherlands, and Division of Medicinal Chemistry, Center for Bio-Pharmaceutical Sciences, P.O. Box 9502, 2300 RA Leiden, The Netherlands

Received December 17, 1993<sup>⊗</sup>

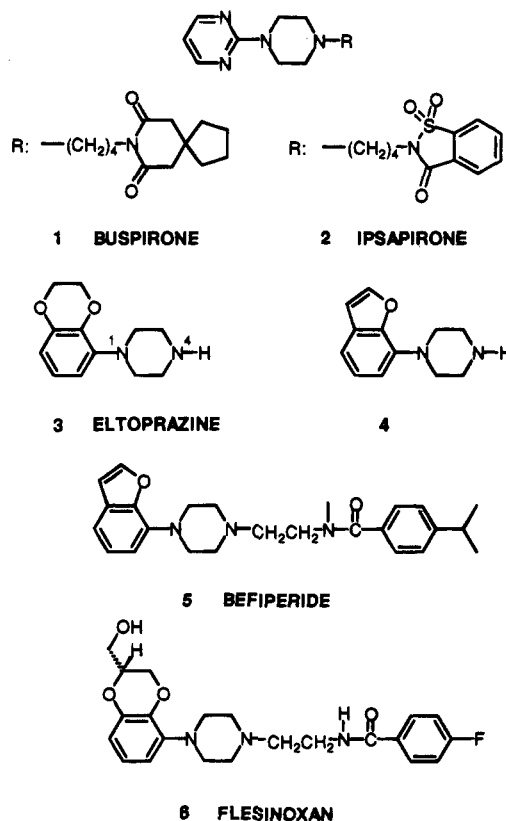
Structure-affinity relationship (SAR) studies for the 5-HT<sub>1A</sub> receptor site are presented for two series of heterobicyclic phenylpiperazines with N4-aralkyl substituents: 4-aralkyl derivatives of 1-(2,3-dihydro-1,4-benzodioxin-5-yl)piperazine (**3**) and 1-(benzo[*b*]furan-7-yl)piperazine (**4**). Their affinities for 5-HT<sub>1A</sub> receptors range from 0.15 to 28 nM and thus emphasize the importance of N4-substitution. By combining the SAR of these N4-aralkyl series with the recently published<sup>11</sup> SAR of the N4-alkyl-substituted phenylpiperazines, the nature of the interaction of the N4-substituted phenylpiperazines and the 5-HT<sub>1A</sub> receptor was further examined using comparative molecular field analysis (CoMFA). To discriminate between two postulated hypotheses, CoMFA models were built and validated utilizing cross-validation, bootstrapping, and randomizing techniques. The model based on a N4-substituent alignment in which all N4-substituents are equally oriented in space was selected for further evaluation. According to the CoMFA/PLS analysis, the steric and electrostatic field properties contribute in a 98:2 ratio to the affinity found for the 5-HT<sub>1A</sub> receptor. Increasing steric bulk was found to be positively as well as negatively related to affinity depending on the distance of the bulk's center from the N4-nitrogen. The location of these steric CoMFA contour levels are well defined in space when the defined alignment rules are followed. Because CoMFA does not take hydrogen bonding into account, this could indicate that the contribution of the amide function (its ability to interact through hydrogen bonding), as present in the N4-substituents, to affinity is of minor importance.

### Introduction

Since the discovery of the neurotransmitter serotonin (5-hydroxytryptamine, 5-HT) in 1948, its role has been associated with many central nervous system (CNS)-related activities. The classification of the multiple types of the 5-HT receptor, their role in various CNS activities, and their respective agonists, partial agonists, and antagonists have been reported in several reviews.<sup>1-4,6,7,9</sup> Of the subtypes known, the 5-HT<sub>1A</sub> receptor is of interest as it is generally accepted that 5-HT<sub>1A</sub> receptors are involved in psychiatric disorders like depression<sup>5</sup> and anxiety.<sup>8,10</sup> Of the different chemical classes which bind to 5-HT<sub>1A</sub> receptors, arylpiperazines such as buspirone (**1**) and ipsapirone (**2**) are effective antianxiety and antidepressant drugs. Evaluation of compounds belonging to another class of arylpiperazines in order to find clinically useful antidepressants, serenics, and anxiolytics led to the discovery of eltoprazine (**3**), its benzofuranyl analogue **4**, befiperide (**5**), and flesinoxan (**6**) (Chart 1).

We recently described the effect of N4-alkylation on the affinity for 5-HT<sub>1A</sub> receptors in two series of heterobicyclic phenylpiperazines: 1-(2,3-dihydro-1,4-benzodioxin-5-yl)piperazine and 1-(benzo[*b*]furan-7-yl)piperazine (Chart 1, compounds **3** (eltoprazine) and **4**).<sup>11</sup> It

Chart 1. Structures of 5-HT<sub>1A</sub> Receptor Ligands



\* To whom correspondence should be addressed at: Solvay Duphar B.V., Department of Medicinal Chemistry, P.O. Box 900, 1380 DA Weesp, The Netherlands. Tel: 31-2940-79602. Fax: 31-2940-10069.

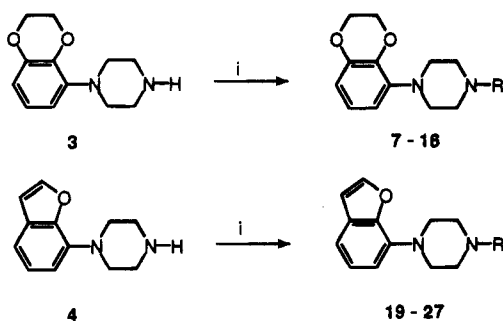
<sup>†</sup> Department of Medicinal Chemistry, Solvay Duphar Research Laboratories.

<sup>‡</sup> Department of Pharmacology, Solvay Duphar Research Laboratories.

<sup>§</sup> Center for Bio-Pharmaceutical Sciences.

<sup>⊗</sup> Abstract published in *Advance ACS Abstracts*, July 15, 1994.

was demonstrated that the N4-alkyl substitution of 1-aryl piperazines significantly influences the ability to

Chart 2<sup>a</sup>

<sup>a</sup> Reagents: (i) RBr, Et<sub>3</sub>N/CH<sub>3</sub>CN (or RCOCl, Et<sub>3</sub>N/CH<sub>3</sub>CN followed by reduction of the amide with LiAlH<sub>4</sub>/THF). Reaction of 4 with *N*-(cyclohexylcarbonyl)aziridine afforded 27.

bind to 5-HT<sub>1A</sub> receptors (Table 3). Hydrocarbon chain substitution up to *N*<sub>4</sub>-propyl shows that *N*-methyl substitution of eltoprazine (3) and its benzofuranyl analogue 4 results in a slight but statistically significant<sup>14</sup> improvement in the affinity. The *N*-ethyl and *N*-propyl derivatives have similar affinities, both being slightly but significantly less active in comparison with the *N*-methyl derivatives. Further elongation of the hydrocarbon chain strongly increases the affinity for 5-HT<sub>1A</sub> receptors, reaching an optimum with the *N*<sub>4</sub>-*n*-hexyl derivatives, e.g., 1-(2,3-dihydro-1,4-benzodioxin-5-yl)-4-*n*-hexylpiperazine (34) has a *K<sub>i</sub>* value of 0.50 nM. Branching of the hydrocarbon chain close to the *N*<sub>4</sub>-nitrogen is unfavorable for high affinity: 1-(2,3-dihydro-1,4-benzodioxin-5-yl)-4-(cyclohexylmethyl)piperazine (9) has a *K<sub>i</sub>* value of 11 nM. Surprisingly, when the cyclohexylmethyl moiety was replaced by cyclohexylethyl, the affinity strongly increased, resulting in a *K<sub>i</sub>* value of 0.25 nM (compound 7, Table 2). Using this cyclohexylethyl derivative as a lead compound, we further investigated this finding. In this paper, the synthesis of a series of cyclohexyl and aralkyl derivatives of eltoprazine (3) and its benzofuranyl analogue 4 and the affinities for 5-HT<sub>1A</sub> receptors obtained by radioligand binding studies is described. Comparative molecular field analysis (CoMFA) was used as a 3-dimensional quantitative structure–affinity relationship (3D-QSAR) method to get more information about the nature of the interaction of the *N*<sub>4</sub>-substituted heterobicyclic phenylpiperazines with the 5-HT<sub>1A</sub> receptor.

## Chemistry

The *N*<sub>4</sub>-aralkylated phenylpiperazines 7–27 were synthesized either by direct alkylation or by reductive alkylation of eltoprazine (3) or its benzofuranyl analogue 4 with the appropriate alkyl halide, alkyl acid chloride, or *N*-acylaziridine (see Chart 2). Physical and spectroscopic properties of the target compounds 7–27 and their intermediates are collected Table 1 and in the Experimental Section. The synthetic methods for the preparation of the key intermediates 3 and 4 were taken from the patent application JP 61,152,655<sup>26</sup> and van Wijngaarden et al.,<sup>11</sup> respectively.

## Results

**Inhibition Constants.** The results of the *in vitro* binding studies in rat frontal cortex homogenates of the target compounds 7–27 measured by displacement of [<sup>3</sup>H]-8-OH-DPAT from its specific binding sites<sup>13</sup> on the 5-HT<sub>1A</sub> receptor are summarized in Table 2.

In order to evaluate the effect of aromaticity in the *N*<sub>4</sub>-chain, the cyclohexylethyl moiety in compound 7 was replaced by a phenethyl group. The resulting phenethyl derivative 8 has a slightly lower affinity for 5-HT<sub>1A</sub> receptors (*K<sub>i</sub>* = 0.47 nM) in comparison with the cyclohexylethyl derivative 7 (*K<sub>i</sub>* = 0.25 nM). When the cyclohexyl moiety in 7 was separated from the *N*<sub>4</sub>-nitrogen by only one methylene group, the affinity decreased significantly (compound 9, *K<sub>i</sub>* = 11 nM). Replacement of the cyclohexyl group in 9 by phenyl resulted in benzyl derivative 10 (*K<sub>i</sub>* = 28 nM), which displays a 2-fold lower affinity in comparison with 9 and is 60 times less potent than its congener 8. When the phenyl group in 8 is separated by four carbon atoms from the *N*<sub>4</sub>-nitrogen atom (compound 11), the affinity slightly but significantly<sup>14</sup> improves, reaching a *K<sub>i</sub>* value of 0.32 nM. Replacement of the methylene group in 11 at position C4 in the chain by oxygen decreases the affinity 3-fold, as demonstrated by the phenoxypropyl derivative 12 (*K<sub>i</sub>* = 0.95 nM). No significant change in affinity was found when the phenoxypropyl group was replaced by a phenoxyethyl group (compound 13, *K<sub>i</sub>* = 0.73 nM). The benzodioxanylethyl derivative 14, which can be regarded as a hybrid of the phenoxyethyl and phenoxypropyl derivatives 12 and 13, respectively, displays a 5-fold lower affinity than the latter compounds. Introduction of a carbonyl group at position C4 in the chain of the phenylbutyl derivative 11 leads to a 2-fold decrease in affinity. There is a further decrease in affinity by 4-fluoro substitution of the phenyl moiety, as shown for compound 16 (*K<sub>i</sub>* = 1.4 nM). Unexpectedly, a 5-fold increase in affinity is found when the carbonyl function in 16 is replaced by a secondary amide function (compound 17). The affinity for 5-HT<sub>1A</sub> receptors of 17 is equal to the affinity found for the phenylbutyl derivative 11. Replacement of the *p*-fluorophenyl moiety of 17 by a cyclohexyl group has only a slight decreasing effect on affinity. The reverse is seen when compounds 7 and 8 and compounds 9 and 10 are compared. Here the affinity of the phenyl compounds is lower than that of the cyclohexyl derivatives. For the benzofuranyl series, the structure–affinity relationship is similar to that of the benzodioxanylethyl series (Table 2).

## Molecular Modeling—Substituent Alignment.

When CoMFA is used with molecules with a large conformational flexibility as in the presented series and, in addition to this, no rigid derivatives are available, the location in space of possible interaction sites can never be determined accurately. But when alignment rules are defined and carefully followed, one can use these CoMFA models as a working hypothesis. It should be stated that these models do not represent a map of the receptor cavity. Furthermore, when CoMFA is used to evaluate SAR studies, normally one set of 3D structures is used. In the present study, we created three sets as described hereafter, representing two basic hypotheses.

The selected conformations and orientations of the *N*<sub>4</sub>-substituents were chosen as outlined below. In our previous publication,<sup>11</sup> we suggested that the nature of the interaction between the *N*<sub>4</sub>-alkyl-substituted phenylpiperazines and the 5-HT<sub>1A</sub> receptor could be a mixture of specific and nonspecific hydrophobic interactions. Of the newly synthesized compounds, the phenylbutyl substituent as present in derivative 11 can be

**Table 1.** Physicochemical Properties and Synthesis Methods of Compounds 7–27

compd	R	formula	prep method <sup>a</sup>	mp (°C)	C, H, N analysis <sup>b</sup>
7	CH <sub>2</sub> CH <sub>2</sub> -(c-C <sub>6</sub> H <sub>11</sub> )	C <sub>26</sub> H <sub>31</sub> N <sub>2</sub> O <sub>2</sub> ·2.00HCl·0.20H <sub>2</sub> O	c	262–4	C, H, N
8	CH <sub>2</sub> CH <sub>2</sub> -C <sub>6</sub> H <sub>5</sub>	C <sub>20</sub> H <sub>24</sub> N <sub>2</sub> O <sub>2</sub> ·1.20HCl	A	242–3	C, H, N
9	CH <sub>2</sub> -(c-C <sub>6</sub> H <sub>11</sub> )	C <sub>19</sub> H <sub>29</sub> N <sub>2</sub> O <sub>2</sub> ·0.30HCl	c	88	C, H, N
10	CH <sub>2</sub> -C <sub>6</sub> H <sub>5</sub>	C <sub>19</sub> H <sub>22</sub> N <sub>2</sub> O <sub>2</sub> ·1.15C <sub>4</sub> H <sub>4</sub> O <sub>4</sub>	B	151	C, H, N
11	(CH <sub>2</sub> ) <sub>4</sub> -C <sub>6</sub> H <sub>5</sub>	C <sub>22</sub> H <sub>22</sub> N <sub>2</sub> O <sub>2</sub> ·2.00HCl	A	218–21	C, H, N
12	(CH <sub>2</sub> ) <sub>3</sub> O-C <sub>6</sub> H <sub>5</sub>	C <sub>21</sub> H <sub>26</sub> N <sub>2</sub> O <sub>3</sub> ·2.00HCl·0.60H <sub>2</sub> O	A	205–8	C, H, N
13	(CH <sub>2</sub> ) <sub>2</sub> O-C <sub>6</sub> H <sub>5</sub>	C <sub>20</sub> H <sub>24</sub> N <sub>2</sub> O <sub>3</sub> ·2.00HCl	A	198–200	C, H, N
14	CH <sub>2</sub> -(benzodioxan-2-yl)	C <sub>21</sub> H <sub>24</sub> N <sub>2</sub> O <sub>4</sub> ·1.50HCl	A	214–8	C, H, N
15	(CH <sub>2</sub> ) <sub>3</sub> CO-C <sub>6</sub> H <sub>5</sub>	C <sub>22</sub> H <sub>26</sub> N <sub>2</sub> O <sub>3</sub> ·2.00HCl·0.30H <sub>2</sub> O	A	212	C, H, N
16	(CH <sub>2</sub> ) <sub>3</sub> CO-C <sub>6</sub> H <sub>4</sub> F	C <sub>22</sub> H <sub>25</sub> F <sub>1</sub> N <sub>2</sub> O <sub>3</sub> ·1.00HCl·0.40H <sub>2</sub> O	A	235–8	C, H, N
17	(CH <sub>2</sub> ) <sub>2</sub> NHCO-C <sub>6</sub> H <sub>4</sub> F	C <sub>21</sub> H <sub>24</sub> F <sub>1</sub> N <sub>3</sub> O <sub>3</sub>	d	170–1	C, H, N
18	(CH <sub>2</sub> ) <sub>2</sub> NHCO-(c-C <sub>6</sub> H <sub>11</sub> )	C <sub>21</sub> H <sub>31</sub> N <sub>3</sub> O <sub>3</sub>	d	155–6	C, H, N
19	CH <sub>2</sub> CH <sub>2</sub> -C <sub>6</sub> H <sub>5</sub>	C <sub>20</sub> H <sub>22</sub> N <sub>2</sub> O <sub>1</sub> ·1.05HCl	A	242–6	C, H, N
20	CH <sub>2</sub> -C <sub>6</sub> H <sub>11</sub>	C <sub>19</sub> H <sub>26</sub> N <sub>2</sub> O <sub>1</sub> ·1.00p-TsOH	c	185–8	C, H, N
21	CH <sub>2</sub> -C <sub>6</sub> H <sub>5</sub>	C <sub>19</sub> H <sub>20</sub> N <sub>2</sub> O <sub>1</sub> ·1.10HCl	A	208–10	C, H, N
22	(CH <sub>2</sub> ) <sub>3</sub> O-C <sub>6</sub> H <sub>5</sub>	C <sub>21</sub> H <sub>24</sub> N <sub>2</sub> O <sub>2</sub> ·1.00HCl	A	165–8	C, H, N
23	(CH <sub>2</sub> ) <sub>2</sub> O-C <sub>6</sub> H <sub>5</sub>	C <sub>20</sub> H <sub>22</sub> N <sub>2</sub> O <sub>2</sub> ·1.00HCl·0.20H <sub>2</sub> O	A	170–6	C, H, N
24	CH <sub>2</sub> -(benzodioxan-2-yl)	C <sub>21</sub> H <sub>22</sub> N <sub>2</sub> O <sub>3</sub>	A	136–40	C, H, N
25	(CH <sub>2</sub> ) <sub>3</sub> CO-C <sub>6</sub> H <sub>4</sub> F	C <sub>22</sub> H <sub>23</sub> N <sub>2</sub> O <sub>2</sub> ·1.00HCl·0.14H <sub>2</sub> O	e	219–20	C, H, N
26	(CH <sub>2</sub> ) <sub>2</sub> NHCO-C <sub>6</sub> H <sub>4</sub> F	C <sub>21</sub> H <sub>22</sub> F <sub>1</sub> N <sub>3</sub> O <sub>2</sub> ·0.20H <sub>2</sub> O	e	157–8	C, H, N
27	(CH <sub>2</sub> ) <sub>2</sub> NHCO-(c-C <sub>6</sub> H <sub>11</sub> )	C <sub>21</sub> H <sub>29</sub> N <sub>3</sub> O <sub>2</sub>	C	183–4	C, H, N

<sup>a</sup> For all compounds, see the Experimental Section. Method A: direct alkylation with the appropriate alkyl halide. Method B: acylation with benzoyl chloride followed by reduction with LiAlH<sub>4</sub>. Method C: reaction with *N*-(cyclohexylcarbonyl)aziridine. <sup>b</sup> All values are within 0.40% of the calculated theoretical values. <sup>c</sup> Compounds 7, 10, and 20 were synthesized as described in ref 2. <sup>d</sup> Compounds 17 and 18 were prepared according to the method described in ref 30. <sup>e</sup> Compounds 25 and 26 were prepared according to the method of van Wijngaarden et al. (ref 1).

**Table 2.** Displacement of [<sup>3</sup>H]-2-(Di-*n*-propylamino)-8-hydroxy-tetralin. Binding to 5-HT<sub>1A</sub> Recognition Sites in Rat Frontal Cortex Homogenates by *N*4-Substituted Heterobicyclic Phenylpiperazines<sup>13</sup>

R	no.	K <sub>i</sub> ± SEM (nM) <sup>a</sup>	no.	K <sub>i</sub> ± SEM (nM)
	7	0.25 ± 0.07		
	8	0.47 ± 0.07	19	0.37 ± 0.11
	9	11 ± 1	20	7.7 ± 0.4
	10	28 ± 5	21	22 ± 5
	11	0.32 ± 0.00		
	12	0.95 ± 0.13	22	0.85 ± 0.1
	13	0.73 ± 0.04	23	0.46 ± 0.03
	14	4.0 ± 0.3	24	5.8 ± 1.3
	15	0.67 ± 0.04		
	16	1.4 ± 0.4	25	1.0 ± 0.3
	17	0.30 ± 0.04	26	0.15 ± 0.01
	18	0.44 ± 0.04	27	0.20 ± 0.03

<sup>a</sup> K<sub>i</sub> ± SEM (nM) values are based on three to six assays, each using four to six concentrations in triplicate.

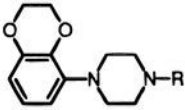
classified as a hydrophobic substituent and therefore will interact in a hydrophobic manner with the receptor. This in contrast to compounds 17 and 26 which bind with an equimolar affinity to the 5-HT<sub>1A</sub> receptor but

in which an amide fragment is present. Due to the presence of this hydrophilic amide function, the interaction of these amide derivatives and the 5-HT<sub>1A</sub> receptor is unlikely to be purely hydrophobic. For these compounds, an additional nonhydrophobic interaction is probably needed in order to explain the high affinity for the 5-HT<sub>1A</sub> receptor. This accessory binding site is presumably of a more hydrophilic nature.

This hydrophobic and hydrophilic interaction site concept was used for further molecular modeling. In order to improve the structural differentiation for the present structure–affinity relationship study, the *N*4-alkyl-substituted derivatives as published previously<sup>11</sup> were also included. These additional linear and branched hydrocarbon chain derivatives of 3 and 4 (see Chart 1) up to the *n*-decyl derivatives with their affinities for the 5-HT<sub>1A</sub> receptor are listed in Table 3.

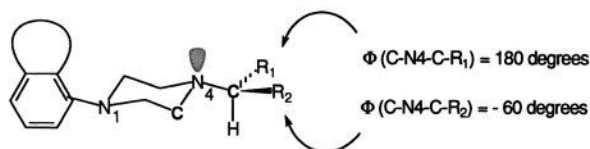
On the basis of the affinity data as presented in Table 2 and 3, two hypotheses about the way the *N*4-substituents interact with the 5-HT<sub>1A</sub> receptor can be postulated. For these two hypotheses, it is assumed that the *N*4-nitrogen atom is the anchor atom in the interaction of the ligands with the 5-HT<sub>1A</sub> receptor site and that the *N*4-substituents are directed toward either the hydrophilic or hydrophobic interaction site.

The first hypothesis is based on the assumption that by adapting one conformation only, both interaction sites can be reached by the compounds. This option results in a model in which all *N*4-substituents are orientated in only one direction. The direction in which the *N*4-substituents are oriented measured from the *N*4-anchor atom was based on the stretched conformations of the *N*4-substituents. These stretched conformations were considered to have a minimum energy conformation. For each compound, the basic 3D coordinates were generated as described in the Experimental Section. After minimization, one of the α-carbon hydrogen atoms in the *N*4-substituent was oriented in space with a “trans” orientation with respect to the *N*4-nitrogen lone pair as shown in Figure 1. Due to this “trans” orientation, this

**Table 3.** Displacement of [<sup>3</sup>H]-2-(Di-*n*-propylamino)-8-hydroxy-tetralin. Binding to Central 5-HT<sub>1A</sub> Recognition Sites in Rat Frontal Cortex Homogenates by *N*4-Alkyl-Substituted Heterobicyclic Phenylpiperazines<sup>13</sup>


R	no.	$K_i \pm \text{SEM}$ (nM) <sup>a</sup>	no.	$K_i \pm \text{SEM}$ (nM) <sup>a</sup>
H	28	40 ± 5	37	13 ± 2
CH <sub>3</sub>	29	24 ± 7	38	8.1 ± 0.6
CH <sub>2</sub> CH <sub>3</sub>	30	66 ± 15	39	23 ± 5
CH <sub>2</sub> CH <sub>2</sub> CH <sub>3</sub>	31	80 ± 11	40	29 ± 2
(CH <sub>2</sub> ) <sub>3</sub> CH <sub>3</sub>	32	12 ± 2	41	5.9 ± 1.2
(CH <sub>2</sub> ) <sub>4</sub> CH <sub>3</sub>	33	2.2 ± 0.4	42	0.81 ± 0.06
(CH <sub>2</sub> ) <sub>5</sub> CH <sub>3</sub>	34	0.50 ± 0.09	43	0.54 ± 0.13
(CH <sub>2</sub> ) <sub>7</sub> CH <sub>3</sub>	35	0.61 ± 0.07	44	1.7 ± 0.4
(CH <sub>2</sub> ) <sub>9</sub> CH <sub>3</sub>	36	1.0 ± 0.3	45	8.0 ± 2.5
CH(CH <sub>3</sub> ) <sub>2</sub>			46	56 ± 17
CH <sub>2</sub> CH(CH <sub>3</sub> ) <sub>2</sub>			47	64 ± 8
CH <sub>2</sub> -( <i>c</i> -C <sub>3</sub> H <sub>5</sub> )			48	20 ± 1
<i>c</i> -C <sub>6</sub> H <sub>11</sub>			49	64 ± 6

<sup>a</sup>  $K_i \pm \text{SEM}$  (nM) values are based on three to six assays, each using four to six concentrations in triplicate. Data taken from van Steen et al. (see ref 11).

**Figure 1.** Schematic representation of the orientation of the *N*4-substituents selected, characterized by the torsion C–*N*4–C–*R*<sub>2</sub> ( $\Phi = -60^\circ$ ) or C–*N*4–C–*R*<sub>1</sub> ( $\Phi = 180^\circ$ ).

alignment is furthermore characterized by the torsion C–*N*4–C–*R*<sub>1</sub> ( $\Phi = 180^\circ$ ). The choice of the torsion  $\Phi = 180^\circ$  (instead of  $\Phi = -60^\circ$ ) for this alignment is random. Following this procedure, for each compound one conformation was built and full geometrical optimization with AM1 was performed. This orientation of the *N*4-substituents and the conformations of all the compounds so obtained are further referred to as alignment set I.

The second hypothesis is based on the possibility that the *N*4-substituent has to adapt a different conformation for each of the interaction sites before interaction with these sites can take place. This option results in a model in which each of the different *N*4-substituents are orientated according to one of two possible directions. Each orientation corresponds with one interaction site. Depending on the chemical structure and properties of the *N*4-substituent, the nature of the interaction with the 5-HT<sub>1A</sub> receptor has to be estimated or chosen in order to create a proper orientation in space. The amide-containing compounds **17**, **18**, **26**, and **27** together with the butyrophenone derivatives **15**, **16**, and **25** were orientated with  $\Phi = -60^\circ$  for the C–*N*4–C–*R*<sub>2</sub> torsion (see Figure 1). The so obtained alignment is defined as the hydrophilic alignment. The term hydrophilic alignment was chosen due to the presence of more hydrophilic substituents. Again, the choice of the direction of the hydrophilic orientation,  $\Phi = -60^\circ$  (instead of  $\Phi = 180^\circ$ ), is random. Non-heteroatom-containing compounds are considered to interact in a hydrophobic manner and thus are orientated with  $\Phi = 180^\circ$  for the torsion C–*N*4–C–*R*<sub>1</sub> (hydrophobic align-

ment). For the sp<sup>3</sup> oxygen-bearing compounds **12–14** and **22–24**, which display a lower affinity than the phenylbutyl-substituted compound **11**, there are two options for interaction. First it is possible that the additional oxygen atom in the phenylbutyl moiety causes a disturbance of the hydrophobic interaction of the phenylbutyl moiety by an additional heteroatom thereby forcing these *N*4-substituents to interact with the hydrophilic interaction site, although in a less favorable way. So these compounds were like the amide- and butyrophenone-containing compounds orientated to the hydrophilic interaction site ( $\Phi = -60^\circ$  for the C–*N*4–C–*R*<sub>2</sub> torsion). The two orientations chosen are schematically presented in Figure 1. The so obtained orientations of the *N*4-substituents is further referred to as alignment set IIa.

Second it is also possible that the decrease in affinity of the sp<sup>3</sup> oxygen-containing compounds is due to a weak interaction with the hydrophobic interaction site. Therefore compounds **12–14** and **22–24** were orientated with  $\Phi = 180^\circ$  for the torsion C–*N*4–C–*R*<sub>1</sub>. The orientation of all the other compounds is conform alignment set IIa. The modification of alignment set IIa is referred to as alignment set IIb.

**Comparative Molecular Field Analysis.** When building models with CoMFA, usually a two-site model is only proposed when the one-site model is insufficient to explain all the data. For the present investigation, this would mean that only the model based on set I would be built and evaluated. By creating the three sets as described in the Molecular Modeling—Substituent Alignment section, we had the opportunity to evaluate the use of CoMFA for the problem of differentiation between the three sets, representing two basic hypotheses.

The three alignment sets I, IIa, and IIb as described above were used in CoMFA to describe the binding affinities (expressed as  $-\log K_i$ ) as a linear function of the corresponding steric and electrostatic field properties. Each of the alignment sets was separately evaluated with CoMFA, and finally all sets were compared. Up to six orthogonal variables were extracted from the partial least-squares (PLS) algorithm as present in the QSAR module of the molecular modeling package SYBYL.<sup>15</sup> For each alignment set (all containing 43 compounds), the CoMFA models were built<sup>31</sup> using a carbon sp<sup>3</sup> atom as the probe atom, having a 1.0 charge. The results of these calculations performed for the three alignment sets are summarized in Table 4. For these initial calculations, CoMFA was used with both the steric and electrostatic fields. Table 4 shows that the models based on the selected alignment sets all have a very high cross-validated  $r^2$  value even for the models built with two components ( $r^2_{cv} > 0.692$ ). These high cross-validated  $r^2$  values suggest a high predictive value for all models based on the selected alignment sets. Using three or more components does not increase the cross-validated  $r^2$  strongly, nor does the  $r^2$  increase more than 5% for an additional component. Therefore a maximum of three components was used for the three alignment sets.<sup>16</sup> Comparing the three sets, alignment set I has the highest cross-validated and conventional  $r^2$  ( $r^2_{cv} = 0.787$  and  $r^2 = 0.919$ , respectively) in comparison with alignment set IIa ( $r^2_{cv} = 0.746$ ,  $r^2 = 0.877$ ) and alignment set IIb ( $r^2_{cv} = 0.740$ ,  $r^2 = 0.871$ ). In order

**Table 4.** CoMFA Models Derived from *N*4-Substituted Heterobicyclic Phenylpiperazine Alignment Sets: Validation Using Bootstrapping Techniques

align set <sup>a</sup>	number of components <sup>b</sup>	<i>r</i> <sup>2</sup> cross <sup>c</sup>	<i>r</i> <sup>2</sup> non-cross <sup>d</sup>	<i>s</i> <sup>e</sup>	<i>r</i> <sup>2</sup> bootstrapped <sup>f</sup>	<i>s</i> bootstrapped <sup>g</sup>
I	2	0.704	0.826	0.361	0.853 ± 0.036	0.322 ± 0.143
	3	0.787	0.919	0.250	0.929 ± 0.020	0.231 ± 0.114
	4	0.822	0.942	0.214	0.957 ± 0.015	0.180 ± 0.101
IIa	2	0.701	0.799	0.388	0.818 ± 0.082	0.364 ± 0.141
	3	0.746	0.877	0.307	0.904 ± 0.027	0.264 ± 0.127
	4	0.781	0.933	0.229	0.948 ± 0.015	0.198 ± 0.101
IIb	2	0.692	0.792	0.395	0.821 ± 0.040	0.362 ± 0.161
	3	0.740	0.871	0.315	0.898 ± 0.025	0.274 ± 0.131
	4	0.772	0.927	0.240	0.943 ± 0.017	0.208 ± 0.107

<sup>a</sup> Alignment set: set I, all compounds were orientated with  $\Phi(\text{C-N4-C-R}_1) = 180^\circ$ ; set IIa, all compounds containing one or more heteroatoms were orientated with  $\Phi(\text{C-N4-C-R}_2) = -60^\circ$ , all others with  $\Phi(\text{C-N4-C-R}_1) = 180^\circ$ ; set IIb, as in set IIa, compounds 12–14 and 22–24 were considered “hydrophobic” ( $\Phi(\text{C-N4-C-R}_1) = 180^\circ$ ). For an explanation of these torsions, see text and Figure 1. <sup>b</sup> Number of components used in CoMFA/PLS run. <sup>c</sup> For all models, the *F*-test value was sufficiently high to result in a zero probability of  $r^2 = 0$ . Validated  $r^2$  values using 43 validation groups. <sup>d</sup> Conventional  $r^2$ . <sup>e</sup> Standard error. <sup>f</sup> Mean and standard deviation of  $r^2$  in 100 bootstrap runs. <sup>g</sup> Mean and standard deviation of *s* in 100 bootstrap runs.

**Table 5.** Validation of CoMFA Models and Alignment Sets Using Randomizing Techniques

align set <sup>a</sup>	number of components <sup>b</sup>	no. of cross <sup>c</sup>	<i>r</i> <sup>2</sup>			score <sup>g</sup>	
			min <sup>d</sup>	avg <sup>e</sup>	max <sup>f</sup>	$r^2 > 0.50$	$r^2 > 0.80$
I	3	0	0.288	0.455	0.644	0.27	0.00
	3	43	-0.723	-0.159	0.241	0.00	0.00
IIa	3	0	0.305	0.465	0.638	0.27	0.00
	3	43	-0.687	-0.165	0.247	0.00	0.00
IIb	3	0	0.291	0.451	0.636	0.17	0.00
	3	43	-0.783	-0.163	0.307	0.00	0.00
random <sup>h</sup>	3	43	0.562	0.646	0.756	1.00	0.00

<sup>a</sup> Alignment set: set I, all compounds were orientated with  $\Phi(\text{C-N4-C-R}_1) = 180^\circ$ ; set IIa, all compounds containing one or more heteroatoms were orientated with  $\Phi(\text{C-N4-C-R}_2) = -60^\circ$ , all others with  $\Phi(\text{C-N4-C-R}_1) = 180^\circ$ ; set IIb, as in set IIa, compounds 12–14 and 22–24 were considered “hydrophobic” ( $\Phi(\text{C-N4-C-R}_1) = 180^\circ$ ). For an explanation of these torsions, see text and Figure 1. <sup>b</sup> Number of components used in CoMFA/PLS run. <sup>c</sup> Number of validation groups. <sup>d</sup> Minimum value of  $r^2$  found after 100 randomizations. <sup>e</sup> Average value of  $r^2$  found after 100 randomizations. <sup>f</sup> Maximum value of  $r^2$  found after 100 randomizations. <sup>g</sup> Fraction of  $r^2 > 0.50$  and  $r^2 > 0.80$  after 100 randomizations. <sup>h</sup> Random: 100 sets in which the torsion  $\Phi(\text{C-N4-C-R}_1/\text{R}_2)$  was randomly distributed as described in the text.

to make a more significant differentiation between the three alignment sets, the confidence intervals (mean and standard deviation of  $r^2$  and the standard error *s*) were determined using the bootstrap technique.<sup>17</sup> The calculated  $r^2$  and *s* as a result of 100 bootstrap runs are summarized in Table 4. Again, extracting more than three components does not increase the cross-validated and conventional  $r^2$  values more than 5% for each additional component, resulting in the optimum number of components being three. Using the bootstrap technique, the three alignment sets were statistically equal as seen from their individual  $r^2$  and standard deviations. The results show that using the bootstrap technique as a validation method, none of the three alignment sets can be selected as the preferred set.

As CoMFA/PLS uses a large number of variables in the calculations, one has to be cautious about the statistical significance of the models derived from CoMFA/PLS.<sup>17–19</sup> In order to evaluate the significance of the models in a more statistical justified manner, we determined the chance correlation of our models by means of randomizing techniques. This chance correlation was determined for the coincidence of the dependent data ( $-\log K_i$ ) being correlated with the steric and electrostatic field and for the coincidence of the selected alignments sets having a high predictive value as illustrated by the high value of the cross-validated  $r^2$ . The results of these chance correlation calculations are summarized in Table 5. For the probability of the  $pK_i$  values being correlated with their corresponding steric and electrostatic fields on the basis of coincidence, we randomized the  $pK_i$  values in the QSAR tables<sup>20</sup> using

the principle of the bootstrapping process. Thus, we randomly selected  $pK_i$  values from the original data set and repeated this selection until the total number of  $pK_i$  values in the new data set reached the size of the original data set, repeated selection of the same  $pK_i$  value being allowed. Using this randomizing technique, 100 data sets were built for alignment sets I, IIa, and IIb in which the original  $pK_i$  values were randomly distributed and the original steric and electrostatic field properties still were present. In all the CoMFA/PLS calculations with these random filled data sets, the number of components varied between two and six. The cross-validated  $r^2$  values was evaluated using three components with 43 cross-validation groups. The results of the validation of the CoMFA models using these data sets are listed in Table 5. The distribution of the conventional and cross-validated  $r^2$  is represented by its minimum, average, and maximum value and its score (fraction of the number of hits) of  $r^2 > 0.50$  and  $r^2 > 0.80$  calculated over 100 runs. Randomizing the dependent data ( $pK_i$ ) as described earlier resulted in remarkably high random conventional  $r^2$  values for the three alignment sets. For a given number of components, the distribution of this  $r^2$  does not show much differentiation. Furthermore, the chance correlation based on the conventional  $r^2$  strongly increases when using additional components. Looking at the predictive value of the alignment sets I, IIa, and IIb (Table 4) in comparison with the random determined predictive value as calculated for three components and 43 cross-validation groups (Table 5), it is clear that the cross-validated  $r^2$  for the three alignments sets is significantly

**Table 6.** Contribution of the Steric and Electrostatic Fields to the Validated and Nonvalidated  $r^2$  Values

align set <sup>a</sup>	number of components <sup>b</sup>	$r^2$ validated (43 groups)			$r^2$ nonvalidated		
		steric + electrostatic <sup>c</sup>	steric <sup>d</sup>	electrostatic <sup>e</sup>	steric + electrostatic	steric	electrostatic
I	3	0.787	0.863	0.626	0.919	0.947	0.860
IIa	3	0.746	0.779	0.393	0.877	0.926	0.807
IIb	3	0.740	0.801	0.557	0.871	0.933	0.810

<sup>a</sup> Alignment set: set I, all compounds were orientated with  $\Phi(\text{C-N4-C-R}_1) = 180^\circ$ ; set IIa, all compounds containing one or more heteroatoms were orientated with  $\Phi(\text{C-N4-C-R}_2) = -60^\circ$ , all others with  $\Phi(\text{C-N4-C-R}_1) = 180^\circ$ ; set IIb, as in set IIa, compounds 12–14 and 22–24 were considered “hydrophobic” ( $\Phi(\text{C-N4-C-R}_1) = 180^\circ$ ). For an explanation of these torsions, see text and Figure 1. <sup>b</sup> Number of components used in CoMFA/PLS run. <sup>c</sup> CoMFA runs using steric and electrostatic fields. <sup>d</sup> CoMFA runs using steric fields only. <sup>e</sup> CoMFA runs using electrostatic fields only.

larger in comparison to the cross-validated  $r^2$  based on coincidence. The maximum found cross-validated  $r^2$  does not exceed 0.241–0.307 for the three randomized alignment sets and is much lower than the original values: 0.740–0.787. This implies that the conventional  $r^2$  is less useful in comparison to the cross-validated  $r^2$  value as a parameter to determine the statistical relevance of the generated CoMFA models. These results are in agreement with the original reason to develop the cross-validation technique. Furthermore, on the basis of the conventional and cross-validated  $r^2$  values, the models derived from alignment sets I, IIa, and IIb are not based on coincidence. Unfortunately, discrimination between the selected alignment sets on the basis of these results is not possible.

The coincidence of alignment sets I, IIa, and IIb having a high predictive value was determined by creating random alignment sets and comparing the cross-validated  $r^2$  value found for alignment sets I, IIa, and IIb with the cross-validated  $r^2$  found for the random alignment sets. These random alignment sets were created as outlined below. As stated earlier, alignment sets IIa and IIb were based on the hypothesis that the N4-substituent has to adapt a different conformation for each of the interaction sites. This option resulted in a model in which each of the different N4-substituents are orientated toward one of two possible directions, as schematically represented in Figure 1. Now, the N4-substituent of each compound was orientated in space, thus that one conformation was built with the torsion  $\text{C-N4-C-R}_2$   $\Phi = -60^\circ$  and one conformation with  $\Phi = 180^\circ$  for the torsion  $\text{C-N4-C-R}_1$ . The random alignment sets were filled with one randomly selected conformer for each compound. Using this procedure, 100 random alignment sets were built and CoMFA/PLS calculations were carried out using two, three, or four components and 43 cross-validation groups. The results of these calculations are summarized in Table 5. It can be seen from Table 5 that the random alignment sets have high cross-validated  $r^2$  values: for three components, the maximum  $r^2_{cv} = 0.756$  and a score of 1.00 for  $r^2_{cv} > 0.50$  was found. When the cross-validated  $r^2$  values of the separate alignment sets I, IIa, and IIb (Table 4) are compared with the randomly found cross-validated  $r^2$  values (Table 5), it can be seen that alignment sets IIa and IIb have  $r^2_{cv}$  values within the random  $r^2_{cv}$  range. This is in contrast to alignment set I with a cross-validated  $r^2 = 0.787$ . These small differences indicate that on the basis of randomizing techniques, alignment set I has the highest  $r^2_{cv}$  value, although chance correlation between the sets I, IIa, and IIb cannot be ruled out.

When the validation of the three sets using cross-validation, bootstrapping, and randomizing techniques

is considered in order to discriminate between the three different sets, it is seen that discrimination is not possible, although the three separate sets show that there is a high degree of correlation between the affinity for the 5-HT<sub>1A</sub> receptor and the corresponding field descriptors.

Finally, the contribution of the steric and electrostatic fields descriptors to the calculated CoMFA models was investigated. All calculations so far were performed using both the steric and electrostatic fields. Now, calculations were run separately with the steric or electrostatic field descriptors for alignment sets I, IIa, and IIb using two to six components and zero or 43 cross-validation groups. The results are summarized in Table 6. For all three alignment sets, the cross-validated  $r^2$  and conventional  $r^2$  values were lower when both field types were used in comparison to the calculations when only the steric field descriptors were used. These results show that the electrostatic field descriptors have a negative effect on the overall cross-validated and conventional  $r^2$  values, suggesting that contribution of the electrostatic field is of minor importance in comparison to the steric descriptors for the statistical parameters of the CoMFA model based on alignment set I. This seems in contrast to the contribution of the separate fields used by CoMFA. When CoMFA is run with both field types, it uses a 53/47 ratio of the steric and electrostatic field descriptors for alignment set I, a 60/40 ratio for alignment set IIa, and a 48/53 ratio for alignment set IIb. All calculations so far were performed using the recommended column-scaling setting COMFA-STD. When no scaling was applied, the ratio found for the steric and electrostatic field contribution was 98/2 for all sets. These results are in agreement with the values found for the CoMFA's run with the separate steric and electrostatic fields, and therefore it seems more appropriate to run further calculations with the TAILOR PLS SCALING setting NONE. The  $r^2_{cv}$  and  $r^2$  values for the nonscaled PLS calculations are 0.863/0.949 (set I), 0.780/0.923 (set IIa), and 0.800/0.932 (set IIb), respectively.

As mentioned before, when building models with CoMFA, a two-site model is only proposed when the one-site model is insufficient to explain all the data. In the present investigation, we have shown that the one-site model which is based on set I shows a high degree of correlation. For these reasons, the one-site CoMFA model derived from alignment set I using three components was further examined. Figure 2 shows the plot of the actual binding affinity versus the predicted binding affinity for the non-cross-validated model. The plot shows that the *n*-decyl derivatives **36** and **45** are outliers: they are the least predictable compounds in the series investigated (**36**,  $\text{p}K_i = 9.00$  versus  $\text{p}K_i = 8.38$ ;

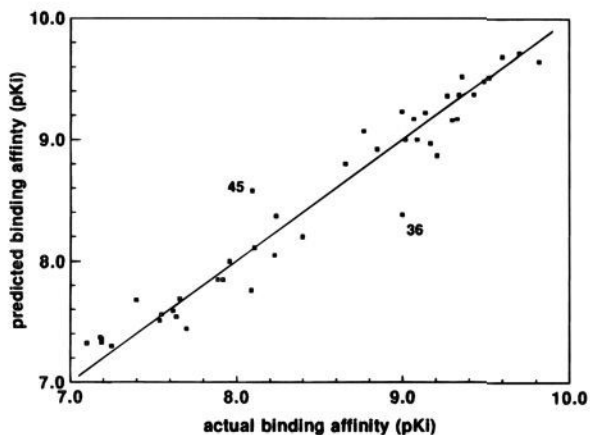


**Figure 2.** Predicted versus actual binding affinity ( $pK_i$  values) for the CoMFA model derived from alignment set I using three components.

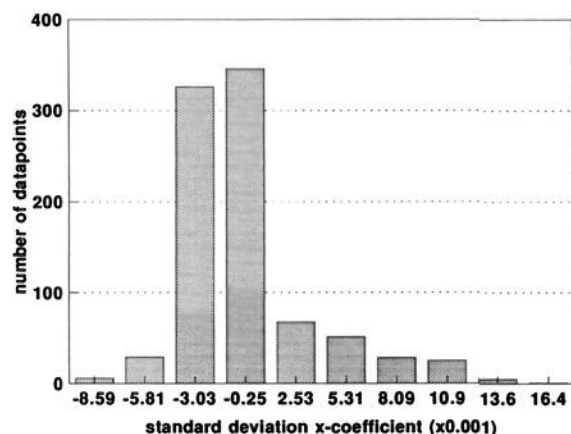


**Figure 3.** Steric field distribution histogram for the CoMFA model based on alignment set I using three components.

45,  $pK_i = 8.10$  versus  $pK_i = 8.58$  for the actual and predicted values, respectively). By omitting 36 and 45 from the data set, the predictive value of the model slightly increases,  $r_{cv}^2 = 0.901$  and  $r^2 = 0.968$  for three components. The long stretched *n*-decyl substituent of 36 and 45 occupies space beyond all the other *N4*-substituents, making it unique. For this reason, CoMFA is not able to correlate the affinity well with the corresponding field descriptors. Due to the relatively small improvement of the model when these derivatives were omitted, they were not excluded from the data set.

From the final model based on alignment set I using all compounds and three components, CoMFA contour maps were generated to better understand the type of information contained in this QSAR model. The statistical parameters of the calculated model can be used for the visualization of the results. The distribution of the standard deviation *x*-coefficient shows where in space differences in the steric bulk and the electrostatic charges are associated with differences in the binding affinity. Contouring these coefficients thus visualizes the 3D areas where steric bulk and electrostatic charge have a positive or negative effect on the affinity. Using the field distribution histograms, the contour levels can be chosen. The steric field distribution histogram is shown in Figure 3. Using this distribution histogram, contour values are chosen which not only have sufficient data points but also have a value which is allocated relatively far away from zero. The so obtained contour

plots show the locations in space where the influence of the field properties on the affinity is largest. The steric field was contoured at the standard deviation *x*-coefficient levels 0.008 and  $-0.004$  as shown in Figure 4. Molecules displayed in Figure 4 are an overlay of compounds 8, 10, 25, 34, 47, and 48. The reason for selecting these compounds is purely illustrative. The compounds are representatives from both series. Figure 4 shows that increasing steric bulk can have a positive as well as negative effect on the affinity. Occupation of space nearby the basic *N4*-nitrogen decreases affinity. When the defined alignment rules are followed, one can give a description of the location of the different field effects. The location of the center of steric bulk occupation where maximum negative effect on affinity is seen can be described by three distance vectors (Figure 5). The first is defined by the distance from the basic *N4*-nitrogen to the center of contour ( $d_{N4} = 3.5 \text{ \AA}$ ) and the second by the distance (measured using the normal) from the plane defined by the *N4*-nitrogen atom, the  $\alpha$ -carbon, and the hydrogen atom attached to this  $\alpha$ -carbon atom of the *N4*-substituent. The distance from this plane (plane(*N4*-C-H)) was found to be  $0.1 \text{ \AA}$ . The third distance is defined by the distance from the plane defined by the *N4*-nitrogen atom, the  $\alpha$ -carbon atom, and the  $\beta$ -carbon atom in the *N4*-substituent. This plane was named plane(*N4*-C- $C_\beta$ ), and the corresponding distance was found to be  $2.3 \text{ \AA}$ . Furthermore, the radius of the half-spherical shaped contour level was measured to be  $1.4 \text{ \AA}$ . For alignment set I, the mentioned  $\beta$ -carbon atom corresponds with the  $R_1$  orientation in Figure 1. Increasing steric bulk shows a positive effect on the affinity when space is occupied further away from the *N4*-nitrogen. The location of this half-sphere-shaped contour level can be described by the center of the sphere, its radius ( $d = 7.3$  and  $2.7 \text{ \AA}$ , respectively) and the distances from the center to the two planes plane(*N4*-C-H) ( $d = 2.3 \text{ \AA}$ ) and plane(*N4*-C- $C_\beta$ ) ( $d = 0.1 \text{ \AA}$ ) as measured by the normals (Figure 5).

Due to the contribution of the steric (98%) and electrostatic field properties (2%), in the final model the electrostatic field was not further examined.

## Discussion

In our previous publication, we suggested that the nature of the interaction between the *N4*-alkyl-substituted phenylpiperazines and the 5-HT<sub>1A</sub> receptor could be a mixture of specific and nonspecific hydrophobic interactions.<sup>11</sup> This conclusion was based on the non-linear SAR found in the *N4*-alkyl series combined with the hydrophobic nature of the substituents investigated. Our current results show that the affinities found for two series of heterobicyclic phenylpiperazines (benzodioxanyl 3 and benzofuranyl 4) with *N4*-aralkyl substituents for 5-HT<sub>1A</sub> receptors can strongly be influenced by the choice of the *N4*-substituents. With the combined *N4*-(ar)alkyl substituent series as presented in this paper, the nature of the interaction of the *N4*-substituted phenylpiperazines and the 5-HT<sub>1A</sub> receptor was further examined using the 3D-QSAR technique CoMFA.

Although in both series *n*-hexyl derivatives have similar  $K_i$  values (34,  $K_i = 0.50 \text{ nM}$ ; 43,  $K_i = 0.54 \text{ nM}$ ; see Table 3), further elongation of the hydrocarbon chain

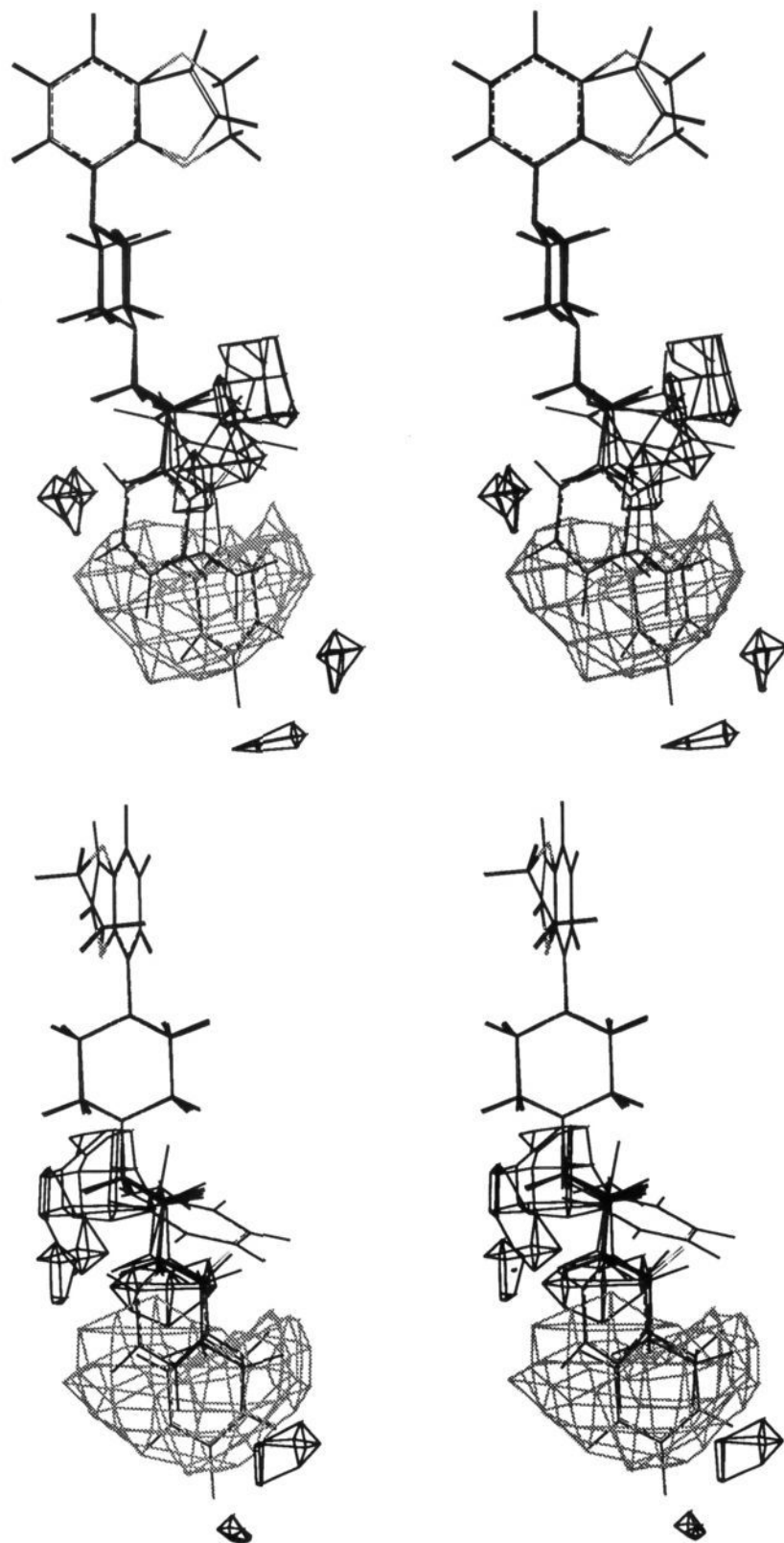


**Figure 4.** (top) Stereoview (crossed) of the CoMFA steric field graph. Contour levels shown correspond with standard deviation  $x$ -coefficient levels of  $-0.004$  (solid lines) and  $0.008$  (dashed lines). The  $-0.004$  contour level is located at  $3.5 \text{ \AA}$  from the basic  $N4$ -nitrogen atom, and an increasing steric bulk in this area negatively influences affinity. The  $0.008$  level is located  $7.3 \text{ \AA}$  from the  $N4$ -nitrogen atom, and an increasing steric bulk in this area positively influences affinity. Molecules displayed are an overlay of compounds **8**, **10**, **25**, **34**, **47**, and **48**. (bottom) Stereoview (crossed) of the CoMFA steric field graph. This view is orthogonal to the view shown above.

in the benzodioxanyl series did not cause a significant decrease in affinity compared to the  $n$ -hexyl compound

as it does in the benzofuranyl series, e.g., the affinities for the  $n$ -decyl derivatives **36** and **45** are 1.0 and 8.0



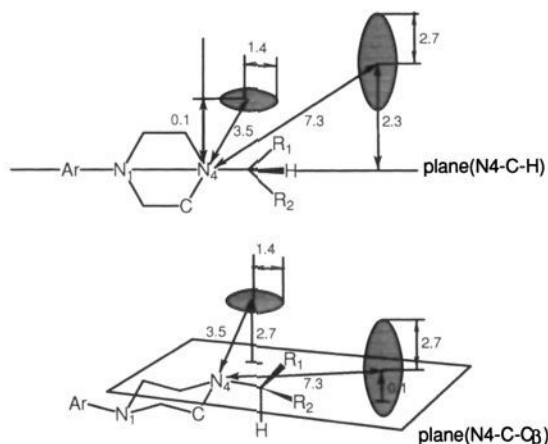


**Figure 5.** Schematic representation of the CoMFA steric field graph, according to the alignment rules as described in the text. Shown are the CoMFA standard deviation  $x$ -coefficient contour levels at  $-0.004$  and  $0.008$ , representing the areas in space where the affinity for the 5-HT<sub>1A</sub> receptor is negatively and positively correlated with the increasing steric bulk of the N4-substituents, respectively. The CoMFA contour levels  $-0.004$  and  $0.008$  are located at a distance 3.5 and 7.3 Å from the N4-nitrogen atom. All distances are in angstroms.

nM, respectively. In the final CoMFA, model compounds **36** and **45** were found to be outliers; they are the least predictable compounds in the series investigated. In contrast to the SAR found for the other substituents investigated, the *n*-decyl derivatives of both series therefore must interact in a different manner with the 5-HT<sub>1A</sub> receptor. In order to further examine this *n*-decyl effect, more compounds with a greater structural differentiation in this 3D area are needed, which are not included in our series.

According to CoMFA, the nature of the interaction between the synthesized ligands and the 5-HT<sub>1A</sub> receptor can be explained by using a 98/2 ratio for the steric versus electrostatic field descriptors in the final model based on alignment set I. This implies that only the steric field plays an important role in the interaction with the 5-HT<sub>1A</sub> receptor for the compounds investigated. The contribution to affinity of increasing steric bulk can be positive as well as negative.

A positive steric bulk contribution is found as a half-sphere-shaped contour level located far from the basic N4-nitrogen atom ( $d = 7.3$  Å) (see Figures 4 and 5). Apparently, when space is occupied according to this contour level, the maximum hydrophobic interaction is reached, resulting in a strong interaction with the 5-HT<sub>1A</sub> receptor site as demonstrated by phenylbutyl derivative **11** ( $K_i = 0.32$  nM).

From Figures 4 and 5, it can also be seen that increasing steric bulk negatively influences the affinity when space is occupied near the basic N4-nitrogen atom ( $d = 3.5$  Å). The effect on affinity can be explained by the steric hindrance caused by certain N4-substituents when the ligands approach the 5-HT<sub>1A</sub> receptor. This affinity-lowering effect could be expected because the N4-nitrogen lone pair is generally accepted to be the major interaction point between the 5-HT<sub>1A</sub> receptor site and the 5-HT<sub>1A</sub> ligands.

The contribution of the steric field descriptors in comparison to the electrostatic field descriptors implies that an increase in hydrophobic properties increases the corresponding interaction for the 5-HT<sub>1A</sub> receptor. In-

deed, when compounds **7** and **8** are compared, the derivative **7** bearing a nonaromatic N4-substituent binds with higher affinity to the 5-HT<sub>1A</sub> receptor. When compounds **9** and **10** or **20** and **21** are compared, a similar effect is seen. However, these compounds display a relatively lower affinity for 5-HT<sub>1A</sub> receptors due to branching of the chain which is less favorable for affinity.<sup>11</sup> The space occupied by these compounds correlates with the location of the area where steric bulk is negatively coupled with affinity according to the CoMFA model.

Introduction of a heteroatom in derivative **11** giving **12** decreases affinity, due to the decrease of the hydrophobic interaction. The hybrid of **12** and **13** (or **22** and **23**) shows a further decrease in affinity resulting in a  $K_i = 4.0$  nM for **14** ( $K_i = 5.8$  nM for the benzofuran hybrid **24**). This decrease in affinity can be explained by a further decrease of the hydrophobic interaction beside an occupation of the area where increasing steric bulk negatively influences affinity due to the geometrical changes as a result from the presence of the additional dioxane ring.

Methylene-carbonyl replacement in **11** to give **15** decreases affinity, which tends to be more pronounced by addition of the electronegative fluorine atom on the phenyl ring in **16**. The amide derivatives **17** and **26** retain high affinity. These SAR effects are not easily explained when CoMFA is considered. The effects indicate that the amide function delocalizes the electronegative charge of the methylene-carbonyl function. Replacement of the *p*-fluorophenyl by a cyclohexyl group decreases affinity due to the loss of the resonance delocalization effect of the *p*-fluorophenyl group on the amide function. In contrast to our first SAR interpretation, the affinity of the amide derivatives **17**, **18**, **26**, and **27** can be fully explained by their steric field properties as used by CoMFA. Because CoMFA does not take hydrogen bonding into account, this could indicate that the contribution of the amide function (in its ability to interact through hydrogen bonding) to affinity is of minor importance. The SAR in these series shows that the evaluation of CoMFA for the present series of compounds gives a more general insight in the field-affinity relationships but that the more specific SAR effects are difficult to extract from the CoMFA model. These difficulties can be a result of the chosen sets or are a limitation of CoMFA when applied to these kinds of sets.

To the best of our knowledge, CoMFA has only been used twice in a structure-affinity/activity relationship study of the 5-HT<sub>1A</sub> receptor. Both publications describe chemical classes other than the heterobicyclic phenylpiperazines. Still some correspondence of the results was found. This does not necessarily imply that the different classes necessarily interact with the 5-HT<sub>1A</sub> receptor in the same way.

Taylor and Agarwal<sup>21</sup> used 3D-QSAR as a structural analysis technique in order to describe the requirements for 5-HT<sub>1A</sub> activity. Using 20 compounds in their model, they extracted no more than five components from the PLS algorithm and concluded that the optimum number of components was five. The predictive value of their model (cross-validated  $r^2$ ) was 0.48, according to the authors, definitely significant. Interestingly, despite the validation of the model, the reported relative contribu-

tion of the steric and electrostatic field descriptors to the final model was found to have a ratio of 94/6. These results are in agreement with the 98/2 field ratio we found in our investigation. The model based on the steric field descriptors alone was much poorer ( $r^2_{cv} = 0.259$ ); thus both fields were used in the final model. Of the 20 compounds used in the CoMFA, six structures had a substituent on the basic nitrogen comparable with our *N*4-substituents. It must be stated that the authors performed a structure-activity relationship study in which CoMFA was used to correlate agonist and antagonist intrinsic activity with the field properties. Therefore the comparison with our structure-affinity relationship study does not necessarily have to be valid.

Langlois<sup>22</sup> performed a structural analysis of 17  $\beta$ -adrenoreceptor blocking agents with 5-HT<sub>1A</sub> and 5-HT<sub>1B</sub> affinity using CoMFA. Unfortunately all the  $\beta$ -adrenoreceptor blocking agents investigated only had isopropyl or *tert*-butyl *N*-substituents, making them even less comparable with our phenylpiperazines.

It can therefore be stated that the present investigation is the first concerning the correlation of 5-HT<sub>1A</sub> receptor affinities with the corresponding steric and electrostatic field properties utilizing heterobicyclic phenylpiperazines with a large structural differentiation in the *N*4-substituents.

## Conclusions

In conclusion, in this paper, we have demonstrated that for two series of heterobicyclic phenylpiperazines (benzodioxanyl **3** and benzofuranyl **4**) with *N*4-aralkyl substituents, the affinity for 5-HT<sub>1A</sub> receptors can be influenced severely by the choice of the *N*4-substituents. The nature of the interaction of the *N*4-substituted phenylpiperazines and the 5-HT<sub>1A</sub> receptor was further examined in the combined *N*4-(ar)alkyl substituent series as presented in our previous paper<sup>11</sup> using CoMFA. To discriminate between the different CoMFA models, cross-validation, bootstrapping, and randomizing techniques were used which showed that no differentiation between the three proposed sets could be made. Since the one-site model shows a high degree of correlation and represents the simplest model, the model derived from alignment set I using three components was further examined. According to the CoMFA/PLS analysis, the steric and electrostatic field properties contribute in a 98/2 ratio to the affinity found for the 5-HT<sub>1A</sub> receptor. The steric bulk was found to be positively as well as negatively related to affinity; the location of the corresponding standard deviation  $x$ -coefficient contour levels is well defined in space. The affinity of the amide derivatives **17**, **18**, **26**, and **27** can be fully explained by their steric field properties as used by CoMFA. Because CoMFA does not take hydrogen bonding into account, this could indicate that the contribution of the amide function (its ability to interact through hydrogen bonding) to affinity is of minor importance.

## Experimental Section

**Molecular Modeling.** The starting coordinates of the 3D structures used were generated using the program CONCORD<sup>23</sup> or the SKETCH option of the molecular modeling software package SYBYL6.0<sup>15</sup> running on Silicon Graphics computers (IRIS 4D/320 and IRIS Indigo ELAN 4000). The energy of the so obtained 3D conformations was minimized

with the Tripos force field using Maximin2, Simplex, and Powell methods. At this time, all methylene groups present in the chain of the *N*4-substituents were oriented to their anti conformation. The orientation of all *N*4-substituents was generated by modifying the C-N4-C-R torsion (see text and Figure 1). These torsional angles were set to  $-60^\circ$  and  $180^\circ$ . This always implied a "trans" orientation of the *N*4-lone pair with respect to the chain  $\alpha$ -CH. Final full geometry optimization was carried out with the semiempirical method AM1 or MOPAC.<sup>24</sup> For these AM1 calculations, the additional keyword "MMOK" was added for compounds **17**, **18**, **26**, and **27**. Finally, all structures were aligned by superimposing of all the phenyl and piperazine *N*4 atoms.

**Comparative Molecular Field Analysis.** For the CoMFA<sup>28</sup> method, we used the 3D-QSAR CoMFA option of SYBYL version 6.0. All molecules were aligned as described in the text. Initially, both steric and electrostatic fields were considered and a region was created where all the molecules under investigation overlapped. A carbon  $sp^3$  atom was used as the probe atom, having a 1.0 charge. The relationship of the steric and electrostatic fields with the biological activity (entered as the  $-\log K_i$  in the CoMFA table) was calculated using the PLS<sup>29</sup> method. Validation and bootstrapping<sup>25</sup> techniques were used to see how well the model predicted the data and to generate confidence limits, respectively. Up to six orthogonal variables were extracted from the linear PLS algorithm. For CoMFA/PLS runs, the SYBYL Tailor setting MINIMUM-SIGMA = 2 was used in a lattice with a 2 Å grid resolution in  $x$ -,  $y$ -, and  $z$ -directions. For the final model, the MINIMUM-SIGMA = 2 was used with a 1 Å grid resolution. Only CoMFA columns were used during the analysis. Initially column scaling was performed using TAILOR PLS SCALING setting COMFA-STD; for the final model evaluation, the TAILOR PLS SCALING setting NONE was used.

**Chemistry.** Melting points are uncorrected. <sup>1</sup>H NMR spectra were recorded on a Bruker WP-200 (200 MHz) or AM400 (400 MHz) instrument. Chemical shifts ( $\delta$ ) are expressed in parts per million relative to internal tetramethylsilane; coupling constants ( $J$ ) are in hertz. Elemental analysis was performed at the TNO laboratory of Organic Chemistry, Utrecht, The Netherlands, and the values were within 0.4% of the theoretical values. Thin-layer chromatography (TLC) was run on Merck silica gel 60 F-254 plates. For normal pressure and flash chromatography, Merck silica gel type 60 (size 70-230 and 230-400 mesh, respectively) was used. Unless stated otherwise, starting materials were used as high-grade commercial products. 1-(2,3-Dihydro-1,4-benzodioxin-5-yl)piperazine, hydrochloride (**3**) and 1-(7-benzofuranyl)piperazine, hydrochloride (**4**) were prepared according to literature procedures (refs 26 and 12, respectively). All reactions were performed under a nitrogen atmosphere.

**1-(Cyclohexylethyl)-4-(2,3-dihydro-1,4-benzodioxin-5-yl)piperazine, Dihydrochloride (7).** Compound **7** was prepared according to the method described by van Steen et al.;<sup>11</sup> yield 21%; mp 262–4 °C; <sup>1</sup>H NMR (CDCl<sub>3</sub>)  $\delta$  0.90–1.90 (cluster, 13 H, cyclohexane and CH<sub>2</sub> cyclohexane), 3.16 (m, 2 H, <sup>+</sup>NHCH<sub>2</sub>CH<sub>2</sub>), 3.60 (m, 4 H, H<sub>eq</sub> CH<sub>2</sub> pip), 4.30–4.55 (cluster, 6 H, 4 H: Bzd H-2,3, and 2 H: H<sub>ax</sub> CH<sub>2</sub> pip), 5.07 (m, 2 H, H<sub>ax</sub> CH<sub>2</sub> pip), 6.93 (t, 1 H, Bzd H-7,  $J = 8$ ), 7.03 (d, 1 H, Bzd H-6,  $J = 8$ ), 7.75 (d, 1 H, Bzd H-8,  $J = 8$ ), 13.55 (br, 1 H, NH<sup>+</sup>). Anal. (C<sub>26</sub>H<sub>31</sub>N<sub>3</sub>O<sub>2</sub>·2.00HCl·0.20H<sub>2</sub>O) C, H, N.

**1-(2,3-Dihydro-1,4-benzodioxin-5-yl)-4-(2-phenylethyl)piperazine, Hydrochloride (8).** To a suspension of **3** (1.47 g, 5.8 mmol) in CH<sub>3</sub>CN (50 mL) was added TEA (2.07 mL, 15.0 mmol) followed by 2-phenylethylbromide (0.74 mL, 5.0 mmol). The solution was heated at reflux for 17 h. After evaporation, the residue was purified by column chromatography (hexane-CH<sub>2</sub>Cl<sub>2</sub>, 2:8). The semisolid was converted to its hydrochloride salt and recrystallized from EtOH: yield 0.85 g (47%); mp 242–3 °C; <sup>1</sup>H NMR free base (CDCl<sub>3</sub>)  $\delta$  2.63–2.89 (cluster, 8 H), 3.12 (br, 4 H, CH<sub>2</sub> pip), 4.25 (m, 2 H, Bzd H-2 or H-3), 4.32 (m, 2 H, Bzd H-2 or H-3), 6.56 (dd, 1 H, Bzd H-6,  $J = 8$  and 2), 6.60 (dd, 1 H, Bzd H-8,  $J = 8$  and 2), 6.78 (t, 1 H, Bzd H-7,  $J = 8$ ), 7.17–7.33 (cluster, 5 H, arom H). Anal. (C<sub>20</sub>H<sub>24</sub>N<sub>2</sub>O<sub>2</sub>·1.20HCl) C, H, N.

**1-(Cyclohexylmethyl)-4-(2,3-dihydro-1,4-benzodioxin-5-yl)piperazine (9).** Compound **9** was prepared according to the method described by van Steen et al.<sup>11</sup> yield 22% of the free base as white crystals; mp 88 °C; <sup>1</sup>H NMR (CDCl<sub>3</sub>) δ 0.82–1.85 (cluster, 11 H, cyclohexane), 2.19 (d, 2 H, NCH<sub>2</sub>CH, *J* = 7), 2.58, 3.08 (br, 4 H, CH<sub>2</sub> pip), 4.24, 4.32 (m, 2 H, Bzd H-2,3), 6.54 (dd, 1 H, Bzd H-6, *J* = 8 and 2), 6.59 (dd, 1 H, Bzd H-8, *J* = 8 and 2), 6.77 (t, 1 H, Bzd H-7, *J* = 8). Anal. (C<sub>19</sub>H<sub>29</sub>N<sub>2</sub>O<sub>2</sub>·0.30H<sub>2</sub>O) C, H, N.

**1-Benzyl-4-(2,3-dihydro-1,4-benzodioxin-5-yl)piperazine, (E)-2-Butenedioate (10).** To LiAlH<sub>4</sub> (0.2 g, 5.26 mmol) suspended in anhydrous THF (20 mL) was added dropwise at 0 °C, **50** (1.4 g, 5.25 mmol) in anhydrous THF (20 mL). After stirring for 6 h at 50 °C and overnight at 20 °C, the mixture was treated cautiously with respectively H<sub>2</sub>O (0.2 mL), 2 N NaOH (0.4 mL), and H<sub>2</sub>O (0.4 mL) at 0 °C. The residue was filtered off over Hyflo after 30 min of stirring at an ambient temperature. The filtrate was washed with H<sub>2</sub>O and evaporated. The solid was purified by column chromatography (THF–MeOH–NH<sub>4</sub>OH, 92:7.5:0.5). The thick oil was converted to its fumaric acid salt: yield 0.56 g (25%); mp 151 °C; <sup>1</sup>H NMR (DMSO–CDCl<sub>3</sub>, 4:1) δ 2.55 (br, 4 H, CH<sub>2</sub> pip), 2.98 (br, 4 H, CH<sub>2</sub> pip), 3.54 (s, 2 H, +NHCH<sub>2</sub>), 4.21 (m, 4 H, Bzd H-2,3), 6.45 (dd, 1 H, Bzd H-6, *J* = 8 and 1), 6.48 (dd, 1 H, Bzd H-8, *J* = 8 and 1), 6.63 (s, 2 H, fumaric acid), 6.69 (t, 1 H, Bzd H-7, *J* = 8), 7.22–7.34 (cluster, 5 H, arom H). Anal. (C<sub>19</sub>H<sub>22</sub>N<sub>2</sub>O<sub>2</sub>·1.15fumarate) C, H, N.

**1-(2,3-Dihydro-1,4-benzodioxin-5-yl)-4-(4-phenylbutyl)-piperazine, Dihydrochloride (11).** Benzenebutanol–methanesulfonate<sup>27</sup> (3.20 g, 14.0 mmol) was dissolved in CH<sub>3</sub>CN (50 mL). **3** (3.25 g, 12.7 mmol) and DIPEA (5.53 mL, 31.8 mmol) were added. The mixture was heated at reflux for 16 h and concentrated after being cooled to 20 °C. The residue was taken up in EtOAc (50 mL) and washed with H<sub>2</sub>O (20 mL). The organic layer was concentrated, and the resulting oil was purified by column chromatography (EtOAc). The obtained product was converted to its dihydrochloride salt: yield 3.30 g (58%); mp 218–21 °C; <sup>1</sup>H NMR (DMSO–CDCl<sub>3</sub>, 4:1) δ 1.63 (m, 2 H, +NHCH<sub>2</sub>CH<sub>2</sub>CH<sub>2</sub>CH<sub>2</sub>), 1.80 (m, 2 H, +NHCH<sub>2</sub>CH<sub>2</sub>CH<sub>2</sub>), 2.64 (t, 2 H, +NHCH<sub>2</sub>CH<sub>2</sub>CH<sub>2</sub>CH<sub>2</sub>, *J* = 8), 3.15 (cluster, 6 H), 3.50 (m, 4 H, CH<sub>2</sub> pip), 4.23 (m, 4 H, Bzd H-2,3), 6.51 (dd, 1 H, Bzd H-6, *J* = 8 and 2), 6.57 (dd, 1 H, Bzd H-8, *J* = 8 and 2), 6.75 (t, 1 H, Bzd H-7, *J* = 8), 7.14–7.32 (cluster, 5 H, arom H), 11.1 (br, 1 H, +NH). Anal. (C<sub>22</sub>H<sub>22</sub>N<sub>2</sub>O<sub>2</sub>·2.00HCl) C, H, N.

**1-(2,3-Dihydro-1,4-benzodioxin-5-yl)-4-(3-phenoxypropyl)piperazine, Dihydrochloride (12).** Compound **12** was prepared from **3** and 3-phenoxypropyl bromide by the method described for **13**: yield 46%; mp 205–8 °C; <sup>1</sup>H NMR (DMSO–CDCl<sub>3</sub>, 4:1) δ 2.29 (m, 2 H, CH<sub>2</sub>CH<sub>2</sub>CH<sub>2</sub>), 3.14–3.29 (cluster, 4 H), 3.32 (m, 2 H, +NHCH<sub>2</sub>CH<sub>2</sub>), 3.52 (m, 2 H, H<sub>eq</sub> CH<sub>2</sub> pip), 3.61 (m, 2 H, H<sub>ax</sub> CH<sub>2</sub> pip), 4.07 (t, 2 H, +NHCH<sub>2</sub>CH<sub>2</sub>CH<sub>2</sub>, *J* = 6), 4.26 (m, 4 H, Bzd H-2,3), 6.51 (dd, 1 H, Bzd H-6, *J* = 8 and 1), 6.56 (dd, 1 H, Bzd H-8, *J* = 8 and 1), 6.74 (t, 1 H, Bzd H-7, *J* = 8), 6.90–6.95 (cluster, 3 H, arom H), 7.27 (m, 2 H, arom H), 11.1 (br, 1 H, +NH). Anal. (C<sub>21</sub>H<sub>26</sub>N<sub>2</sub>O<sub>3</sub>·2.00HCl·0.60H<sub>2</sub>O) C, H, N.

**1-(2,3-Dihydro-1,4-benzodioxin-5-yl)-4-(2-phenoxyethyl)piperazine, Dihydrochloride (13).** 2-Phenoxyethyl bromide (4.70 g, 23.4 mmol), **3** (5.00 g, 19.5 mmol), DIPEA (8.50 mL, 48.8 mmol), and NaI (0.1 g, catalytic) were dissolved in CH<sub>3</sub>CN (50 mL) and heated at reflux for 16 h. After evaporation of the volatiles, the residue was taken up in EtOAc (50 mL) and washed with H<sub>2</sub>O (2 × 15 mL). The organic layer was dried (Na<sub>2</sub>SO<sub>4</sub>) and concentrated. The obtained product was converted to its dihydrochloride salt and recrystallized from EtOH: yield 3.5 g (43%); mp 198–200 °C; <sup>1</sup>H NMR (DMSO–CDCl<sub>3</sub>, 4:1) δ 3.20 (m, 2 H, H<sub>ax</sub> CH<sub>2</sub> pip), 3.37 (m, 2 H, H<sub>ax</sub> CH<sub>2</sub> pip), 3.52 (m, 2 H, H<sub>eq</sub> CH<sub>2</sub> pip), 3.60–3.70 (cluster, 4 H), 4.21–4.30 (cluster, 4 H, Bzd H-2,3), 4.50 (t, 2 H, +NHCH<sub>2</sub>CH<sub>2</sub>, *J* = 5), 6.50 (dd, 1 H, Bzd H-6, *J* = 8 and 1), 6.57 (dd, 1 H, Bzd H-8, *J* = 8 and 1), 6.75 (t, 1 H, Bzd H-7, *J* = 8), 6.96–7.03 (cluster, 3 H, arom H), 7.30 (m, 2 H, arom H), 11.5 (br, 1 H, +NH). Anal. (C<sub>20</sub>H<sub>24</sub>N<sub>2</sub>O<sub>3</sub>·2.00HCl) C, H, N.

**1-[(2,3-Dihydro-1,4-benzodioxin-2-yl)methyl]-4-(2,3-dihydro-1,4-benzodioxin-5-yl)piperazine, Hydrochloride**

(14). Compound **14** was prepared from **3** and 2-(bromomethyl)-2,3-dihydro-1,4-benzodioxin by the method described for **16**. Reflux time was 60 h. Purification was by column chromatography (CH<sub>2</sub>Cl<sub>2</sub>–hexane, 8:2). The obtained product was converted to its hydrochloride salt: yield 22%; mp 214–8 °C; <sup>1</sup>H NMR free base (CDCl<sub>3</sub>) δ 2.61–2.86 (cluster, 6 H), 3.09 (m, 4 H, CH<sub>2</sub> pip), 4.02 (dd, 1 H, Bzd H-3, *J* = 12 and 8), 4.25 (m, 2 H, Bzd H-2 or H-3), 4.29–4.40 (cluster, 4 H), 6.54 (dd, 1 H, Bzd H-6, *J* = 8 and 1), 6.60 (dd, 1 H, Bzd H-8, *J* = 8 and 1), 6.78 (t, 1 H, Bzd H-7, *J* = 8), 6.81–6.93 (cluster, 4 H). Anal. (C<sub>21</sub>H<sub>24</sub>N<sub>2</sub>O<sub>4</sub>·1.50HCl) C, H, N.

**4-[4-(2,3-Dihydro-1,4-benzodioxin-5-yl)-1-piperazinyl]-1-phenyl-1-butanone, Dihydrochloride (15).** To a solution of **3** (4.5 g, 17.5 mmol) and 4-chlorobutyrophenone (4.0 g, 21.9 mmol) in DMF (250 mL) were added DIPEA (3.75 mL, 21.5 mmol) and NaI (2.6 g, 17.3 mmol). After stirring for 16 h at 90 °C, the reaction mixture was concentrated in vacuo. The residue was taken up in EtOAc (50 mL) and washed with H<sub>2</sub>O (15 mL). The EtOAc was removed in vacuo, and the resulting crude oil was purified by column chromatography (THF–MeOH–NH<sub>4</sub>OH, 97.5:2.5:0.15). The resulting product was converted to its dihydrochloride salt: yield 3.06 g (40%); mp 212 °C; <sup>1</sup>H NMR (DMSO–CDCl<sub>3</sub>, 4:1) δ 2.13 (m, 2 H, CH<sub>2</sub>CH<sub>2</sub>CH<sub>2</sub>), 3.07–3.28 (cluster, 8 H), 3.53 (m, 2 H, H<sub>eq</sub> CH<sub>2</sub> pip), 3.61 (m, 2 H, H<sub>ax</sub> CH<sub>2</sub> pip), 4.25 (m, 4 H, Bzd H-2,3), 6.51 (dd, 1 H, Bzd H-6, *J* = 8 and 1), 6.57 (dd, 1 H, Bzd H-8, *J* = 8 and 1), 6.75 (t, 1 H, Bzd H-7, *J* = 8), 7.53 (m, 2 H, arom H), 7.64 (m, 1 H, arom H), 8.00 (m, 2 H, arom H), 10.55 (br, 1 H, +NH). Anal. (C<sub>22</sub>H<sub>26</sub>N<sub>2</sub>O<sub>3</sub>·2.00HCl·0.30H<sub>2</sub>O) C, H, N.

**4-[4-(2,3-Dihydro-1,4-Benzodioxin-5-yl)-1-piperazinyl]-1-(4-fluorophenyl)-1-butanone, Hydrochloride (16).** 4-Chloro-4'-fluorobutyrophenone (1.63 mL, 10.0 mmol), the free base of **3** (2.2 g, 10.0 mmol), and TEA (1.4 mL, 10.0 mmol) were stirred for 18 h at 60 °C. After the solution had cooled to 20 °C, THF (40 mL) was added and TEA·HCl was filtered off over Hyflo. The filtrate was concentrated in vacuo, and the free base of **16** was converted to its monohydrochloride salt. The solid was recrystallized from isopropyl alcohol (75 mL): yield 1.18 g (28%); mp 235–8 °C; <sup>1</sup>H NMR (DMSO–CDCl<sub>3</sub>, 4:1) δ 2.12 (m, 2 H, CH<sub>2</sub>CH<sub>2</sub>CH<sub>2</sub>), 3.08–3.27 (cluster, 8 H), 3.52 (m, 2 H, H<sub>eq</sub> CH<sub>2</sub> pip), 3.60 (m, 2 H, H<sub>ax</sub> CH<sub>2</sub> pip), 4.25 (m, 4 H, Bzd H-2,3), 6.51 (dd, 1 H, Bzd H-6, *J* = 8 and 1), 6.57 (dd, 1 H, Bzd H-8, *J* = 8 and 1), 6.75 (t, 1 H, Bzd H-7, *J* = 8 and 1), 6.75 (t, 1 H, Bzd H-7, *J* = 8), 7.32 (m, 2 H, arom H), 8.08 (m, 2 H, arom H), 10.75 (br, 1 H, +NH). Anal. (C<sub>22</sub>H<sub>25</sub>F<sub>1</sub>N<sub>2</sub>O<sub>3</sub>·1.00HCl·0.40H<sub>2</sub>O) C, H, N.

**N-[2-[4-(2,3-Dihydro-1,4-Benzodioxin-5-yl)-1-piperazinyl]ethyl]-4-fluorobenzamide (17).** Compound **17** was prepared according to the method as described in ref 30: yield 18%; mp 170–1 °C; <sup>1</sup>H NMR (CDCl<sub>3</sub>) δ 2.70 (cluster, 6 H, CH<sub>2</sub> pip and NCH<sub>2</sub>CH<sub>2</sub>), 3.1 (m, 4 H, CH<sub>2</sub> pip), 3.58 (q, 2 H, O=CNHCH<sub>2</sub>CH<sub>2</sub>, *J* = 6), 4.28 (m, 4 H, Bzd H-2,3), 6.54 (dd, 1 H, Bzd H-6, *J* = 8 and 1), 6.61 (dd, 1 H, Bzd H-8, *J* = 8 and 1), 6.79 (t, 1 H, Bzd H-7, *J* = 8), 6.86 (br t, 1 H, O=CNHCH<sub>2</sub>), 7.12 (m, 2 H, arom H), 7.80 (m, 2 H, arom H). Anal. (C<sub>21</sub>H<sub>24</sub>F<sub>1</sub>N<sub>3</sub>O<sub>3</sub>) C, H, N.

**N-[2-[4-(2,3-Dihydro-1,4-benzodioxin-5-yl)-1-piperazinyl]ethyl]cyclohexanecarboxamide (18).** Compound **18** was prepared according to the method as described in ref 30: yield 56%; mp 155–6.0 °C; <sup>1</sup>H NMR (CDCl<sub>3</sub>) δ 1.14–1.92 (cluster, 10 H, cyclohexyl), 2.10 (m, 1 H, H<sub>ax</sub> cyclohexyl), 2.55 (t, 2 H, NCH<sub>2</sub>CH<sub>2</sub>, *J* = 6), 2.75 (br, 4 H, CH<sub>2</sub> pip), 3.08 (br, 4 H, CH<sub>2</sub> pip), 3.37 (q, 2 H, O=CNHCH<sub>2</sub>CH<sub>2</sub>), 4.29 (m, 4 H, Bzd H-2,3), 6.10 (br t, 1 H, O=CNHCH<sub>2</sub>), 6.55 (dd, 1 H, Bzd H-6, *J* = 8 and 1), 6.61 (dd, 1 H, Bzd H-8, *J* = 8 and 1), 6.78 (t, 1 H, Bzd H-7, *J* = 8). Anal. (C<sub>21</sub>H<sub>31</sub>N<sub>3</sub>O<sub>3</sub>) C, H, N.

**1-(7-Benzofuranyl)-4-(2-phenylethyl)piperazine, Hydrochloride (19).** Compound **19** was prepared from **3** and 2-phenoxyethyl bromide by the method described for **13**. Reflux time was 16 h: yield 68%; mp 242–6 °C; <sup>1</sup>H NMR (DMSO–CDCl<sub>3</sub>, 4:1) δ 3.1–4.1 (br, 12 H), 6.82 (dd, 1 H, Bzf H-6, *J* = 8 and 1), 6.89 (d, 1 H, Bzf H-3, *J* = 2), 7.16 (t, 1 H, Bzf H-5, *J* = 8), 7.2–7.4 (cluster, 6 H, arom H and Bzf H-4), 7.89 (d, 1 H, Bzf H-2, *J* = 2), 11.56 (br, 1 H, +NH). Anal. (C<sub>20</sub>H<sub>22</sub>N<sub>2</sub>O<sub>3</sub>·1.05HCl) C, H, N.

**1-(7-Benzofuranyl)-4-(cyclohexylmethyl)piperazine, p-Toluenesulfonate (20).** Compound **20** was prepared accord-

ing to the method described by van Steen et al.<sup>11</sup> yield 38%; mp 185–8 °C; <sup>1</sup>H NMR (CDCl<sub>3</sub>) δ 1.01–1.92 (cluster, 11 H, cyclohexane), 2.33 (s, 3H, CH<sub>3</sub> tosylaat), 2.97 (t, 2 H, <sup>+</sup>NHCH<sub>2</sub>CH, *J* = 6), 3.11, 3.66 (m, 2 H, H<sub>ax</sub> CH<sub>2</sub> pip), 3.80 (m, 4 H, H<sub>eq</sub> CH<sub>2</sub> pip), 6.74 (d, 1 H, Bzf H-6, *J* = 8), 6.77 (d, 1 H, Bzf H-3, *J* = 2), 7.15 (cluster, 3 H, 1 H: Bzf H-5, and 2 H: tosylaat), 7.29 (d, 1 H, Bzf H-4, *J* = 8), 7.59 (d, 1 H, Bzf H-2, *J* = 2), 7.77 (m, 2 H, tosylaat), 10.8 (br, 1 H, NH<sup>+</sup>). Anal. (C<sub>19</sub>H<sub>26</sub>N<sub>2</sub>O<sub>1</sub>·1.00p-TsOH) C, H, N.

**1-(7-Benzofuranyl)-4-benzylpiperazine, Hydrochloride (21).** To a stirred suspension of **4** (1.46 g, 6.12 mmol) in CH<sub>3</sub>CN (25 mL) were added benzyl bromide (1.02 mL, 8.60 mmol) and DIPEA (2.14 mL, 12.3 mmol). A yellow solution was formed. After the solution was heated to reflux for 3 h, all volatiles were removed in vacuo. The residue was purified by column chromatography (CH<sub>2</sub>Cl<sub>2</sub>–MeOH, 96:4). The obtained oil was taken up in ether (50 mL) and washed with 2 N NaOH (15 mL); the organic layer was dried (Na<sub>2</sub>SO<sub>4</sub>) and concentrated. The obtained free base was converted to its hydrochloride salt: yield 1.28 g (64%); mp 208–210 °C; <sup>1</sup>H NMR (CDCl<sub>3</sub>) δ 3.14 (br, 2 H, CH<sub>2</sub> pip), 3.54 (br, 2 H, H<sub>eq</sub> CH<sub>2</sub> pip), 3.65–3.86 (cluster, 4 H, CH<sub>2</sub> pip), 4.28 (s, 2 H, <sup>+</sup>NHCH<sub>2</sub>), 6.73 (d, 1 H, Bzf H-6, *J* = 8), 6.75 (d, 1 H, Bzf H-3, *J* = 2), 7.13 (t, 1 H, Bzf H-5, *J* = 8), 7.26 (d, 1 H, Bzf H-4, *J* = 8), 7.45 (3 H, arom H), 7.55 (d, 1 H, Bzf H-2, *J* = 2), 7.70 (2 H, arom H), 12.95 (br, 1 H, <sup>+</sup>NH). Anal. (C<sub>19</sub>H<sub>20</sub>N<sub>2</sub>O<sub>1</sub>·1.10HCl) C, H, N.

**1-(7-Benzofuranyl)-4-(3-phenoxypropyl)piperazine, Hydrochloride (22).** Compound **22** was prepared from **4** and 3-phenoxypropyl bromide by the method described for **23**. Reflux time was 3 h, and purification was by flash chromatography (CH<sub>2</sub>Cl<sub>2</sub>–MeOH, 98:2): yield 75%; mp 165–8 °C; <sup>1</sup>H NMR (CDCl<sub>3</sub>) δ 2.50 (m, 2 H, CH<sub>2</sub>CH<sub>2</sub>CH<sub>2</sub>), 3.48–3.98 (cluster, 10 H, CH<sub>2</sub> pip and <sup>+</sup>NHCH<sub>2</sub>CH<sub>2</sub>), 4.08 (t, 2 H, <sup>+</sup>NHCH<sub>2</sub>CH<sub>2</sub>CH<sub>2</sub>, *J* = 5), 6.76 (d, 1 H, Bzf H-6, *J* = 8), 6.77 (d, 1 H, Bzf H-3, *J* = 2), 6.87 (m, 2 H, arom H), 6.96 (m, 1 H, arom H), 7.14 (t, 1 H, Bzf H-5, *J* = 8), 7.21–7.36 (cluster, 3 H), 7.58 (d, 1 H, Bzf H-2, *J* = 2), 12.8 (br, 1 H, <sup>+</sup>NH). Anal. (C<sub>21</sub>H<sub>24</sub>N<sub>2</sub>O<sub>2</sub>·1.00HCl) C, H, N.

**1-(7-Benzofuranyl)-4-(2-phenoxyethyl)piperazine, Hydrochloride (23).** To a stirred suspension of **4** (1.50 g, 6.28 mmol) in CH<sub>3</sub>CN (25 mL) were added 2-phenoxyethyl bromide (1.77 g, 8.80 mmol) and DIPEA (2.19 mL, 12.86 mmol). After being heated to reflux for 18 h, the mixture was concentrated and purified by column chromatography (CH<sub>2</sub>Cl<sub>2</sub>–MeOH, 96:4). The oily product was taken up in EtOAc (25 mL) and washed twice with 2 N NaOH (10 mL) to remove the formed carbonate salt. The organic layer was dried (Na<sub>2</sub>SO<sub>4</sub>) and concentrated yielding the free base of **23**. Conversion to its HCl salt was carried out in light petroleum ether (30 mL) by the addition of 1 equiv of HCl in methanol (5 mL). After cooling to –15 °C, the formed crystals were collected on a filter and dried at ambient temperature under reduced pressure to yield 1.60 g (73%): mp 170–6 °C; <sup>1</sup>H NMR (CDCl<sub>3</sub>) δ 3.62 (br, 2 H, <sup>+</sup>NHCH<sub>2</sub>CH<sub>2</sub>), 3.75–4.05 (cluster, 6 H, CH<sub>2</sub> pip), 4.34 (m, 2 H, CH<sub>2</sub> pip), 4.63 (br, 2 H, <sup>+</sup>NHCH<sub>2</sub>CH<sub>2</sub>), 6.84 (d, 1 H, Bzf H-3, *J* = 2), 6.88–7.08 (cluster, 3 H, arom H), 7.23 (t, 1 H, Bzf H-5, *J* = 8), 7.30 (t, 2 H, arom H), 7.42 (d, 1 H, Bzf H-6, *J* = 8), 7.50 (d, 1 H, Bzf H-4, *J* = 8), 7.72 (d, 1 H, Bzf H-2, *J* = 2), 13.66 (br, 1 H, <sup>+</sup>NH). Anal. (C<sub>20</sub>H<sub>22</sub>N<sub>2</sub>O<sub>2</sub>·1.00HCl·0.20H<sub>2</sub>O) C, H, N.

**1-(7-Benzofuranyl)-4-[(2,3-dihydro-1,4-benzodioxin-2-yl)methyl]piperazine (24).** To a solution of the free base of **4** (1.2 g, 5.94 mmol) in DMF (15 mL) were added 2-(chloromethyl)-2,3-dihydro-1,4-benzodioxin (1.1 g, 5.96 mmol), NaHCO<sub>3</sub> (0.53 g, 6.3 mmol), and NaI (0.9 g, 6.00 mmol). After the mixture had stirred for 55 h at 80 °C, CH<sub>2</sub>Cl<sub>2</sub> (100 mL) was added. The solution was washed with H<sub>2</sub>O (3 × 15 mL) and NaOH (15 mL), dried (MgSO<sub>4</sub>), and concentrated in vacuo. The residue was purified by column chromatography (CH<sub>2</sub>Cl<sub>2</sub>–MeOH, 99:1) giving 1.33 g (64%) of a solid, which was crystallized from EtOAc (10 mL). White crystals were filtered off, washed with light petroleum ether, and dried in vacuo at 40 °C: yield 0.8 g (38%); mp 136–40 °C; <sup>1</sup>H NMR (CDCl<sub>3</sub>) δ 2.62–2.98 (cluster, 6 H), 3.38 (m, 4 H, CH<sub>2</sub> pip), 4.05 (dd, 1 H, Bzd H-3, *J* = 12 and 8), 4.30–4.48 (cluster, 2 H), 6.72–6.98 (cluster, 6 H), 7.18 (t, 1 H, Bzf H-5, *J* = 8), 7.23 (dd, 1 H, Bzf

H-4, *J* = 8 and 1), 7.62 (d, 1 H, Bzf H-2, *J* = 2). Anal. (C<sub>21</sub>H<sub>22</sub>N<sub>2</sub>O<sub>3</sub>) C, H, N.

**4-[4-(7-Benzofuranyl)-1-piperazinyl]-1-(4-fluorophenyl)-1-butanone, Hydrochloride (25).** Compound **25** was prepared by the procedure of van Wijngaarden et al.<sup>12</sup> yield 33%; mp 219–220 °C; <sup>1</sup>H NMR (CDCl<sub>3</sub>) δ 2.41 (m, 2 H, CH<sub>2</sub>CH<sub>2</sub>CH<sub>2</sub>), 3.07–3.32 (cluster, 6 H), 3.64–3.95 (cluster, 6 H), 6.79 (cluster, 2 H, Bzf H-3,6), 7.15 (cluster, 3 H, Bzf H-5 and FAr H-3,5), 7.29 (d, 1 H, Bzf H-4, *J* = 8), 7.60 (d, 1 H, Bzf H-2, *J* = 2), 8.01 (dd, 2 H, FAr H-2,6, *J* = 5 and 8), 12.7 (br, 1 H, <sup>+</sup>NH). Anal. (C<sub>22</sub>H<sub>23</sub>F<sub>1</sub>N<sub>2</sub>O<sub>2</sub>·1.00HCl·0.14H<sub>2</sub>O) C, H, N.

**N-[2-[4-(7-Benzofuranyl)-1-piperazinyl]ethyl]-4-fluorobenzamide (26).** Compound **26** was prepared by the procedure of van Wijngaarden et al.<sup>12</sup> yield 71%; mp 157–8 °C; <sup>1</sup>H NMR (CDCl<sub>3</sub>) δ 2.71 (t, 2 H, NCH<sub>2</sub>CH<sub>2</sub>, *J* = 6), 2.77 (m, 4 H, CH<sub>2</sub> pip), 3.39 (m, 4 H, CH<sub>2</sub> pip), 3.61 (q, 2 H, O=CNHCH<sub>2</sub>CH<sub>2</sub>, *J* = 6), 6.76 (d, 1 H, Bzf H-3, *J* = 2), 6.78 (dd, 1 H, Bzf H-6, *J* = 8 and 1), 6.84 (br t, 1 H, CH<sub>2</sub>NHC=O, *J* = 6), 7.12 (m, 2 H, FAr H-3,5), 7.16 (t, 1 H, Bzf H-5, *J* = 8), 7.24 (dd, 1 H, Bzf H-4, *J* = 8 and 1), 7.62 (d, 1 H, Bzf H-2, *J* = 2), 7.81 (m, 2 H, FAr H-2,6). Anal. (C<sub>21</sub>H<sub>22</sub>F<sub>1</sub>N<sub>3</sub>O<sub>2</sub>·0.20H<sub>2</sub>O) C, H, N.

**N-[2-[4-(7-Benzofuranyl)-1-piperazinyl]ethyl]cyclohexanecarboxamide (27).** (a) Aziridine (12.82 g, 0.30 mol) in CH<sub>2</sub>Cl<sub>2</sub> (90 mL) was added to a cooled (5 °C) solution of NaOH (12.0 g, 0.30 mol) in H<sub>2</sub>O (75 mL). Cyclohexanecarboxylic acid chloride (43.7 g, 0.30 mol) in CH<sub>2</sub>Cl<sub>2</sub> (90 mL) was added dropwise at –10 °C. The two layers were separated, and the water layer was extracted with CH<sub>2</sub>Cl<sub>2</sub> (25 mL). The combined organic layers were dried (MgSO<sub>4</sub>) and concentrated: yield 43.6 g (95%) of *N*-(cyclohexylcarbonyl)aziridine; colorless oil; <sup>1</sup>H NMR (CDCl<sub>3</sub>) δ 1.1–2.0 (cluster, 10 H, cyclohexyl), 2.21 (s, 4 H, aziridine), 2.44 (m, 1 H, cyclohexyl).

(b) The free base of **4** (5.00 g, 24.8 mmol) and *N*-(cyclohexylcarbonyl)aziridine (4.00 g, 26.0 mmol) were heated at 80 °C under reduced pressure (15 mmHg). After 30 min, CH<sub>3</sub>CN (100 mL) was added and the formed solid was stirred for 60 min. The white crystals were collected on a filter and dried at ambient temperature under reduced pressure to yield 8.60 g (98%): mp 183–4 °C; <sup>1</sup>H NMR (CDCl<sub>3</sub>) δ 1.15–1.35 (cluster, 3 H, H<sub>ax</sub> cyclohexyl), 1.44 (m, 2 H, H<sub>ax</sub> cyclohexyl), 1.67 (m, 1 H, H<sub>eq</sub> cyclohexyl), 1.79 (m, 2 H, H<sub>eq</sub> cyclohexyl), 1.87 (m, 2 H, H<sub>eq</sub> cyclohexyl), 2.11 (m, 1 H, H<sub>ax</sub> cyclohexyl), 2.58 (t, 2 H, NCH<sub>2</sub>CH<sub>2</sub>, *J* = 5), 2.72 (m, 4 H, CH<sub>2</sub> pip), 3.31–3.44 (cluster, 6 H), 6.08 (br t, 1 H, O=CNHCH<sub>2</sub>, *J* = 5), 6.75 (d, 1 H, Bzf H-3, *J* = 2), 6.78 (dd, 1 H, Bzf H-6, *J* = 8 and 1), 7.16 (t, 1 H, Bzf H-5, *J* = 8), 7.22 (dd, 1 H, Bzf H-4, *J* = 8 and 1), 7.61 (d, 1 H, Bzf H-2, *J* = 2). Anal. (C<sub>21</sub>H<sub>29</sub>N<sub>3</sub>O<sub>2</sub>) C, H, N.

**1-Benzoyl-4-(2,3-dihydro-1,4-benzodioxin-5-yl)piperazine (50).** To a solution of the free base of **3** (2.20 g, 10.0 mmol) in CH<sub>3</sub>CN (30 mL) were added TEA (1.5 mL, 10.8 mmol) and benzoyl chloride (1.16 mL, 10.0 mmol). After the solution had stirred for 30 min at 20 °C, the precipitate was filtered off and the filtrate was concentrated in vacuo. The white solid, which still contained TEA·HCl, was taken up in ether (100 mL). After the solution was heated at reflux for 10 min, the TEA·HCl was filtered off and the filtrate was concentrated in vacuo giving **50** as a white solid: yield 1.9 g (59%); mp 137 °C; <sup>1</sup>H NMR (CDCl<sub>3</sub>) δ 3.00, 3.13, 3.61, 3.97 (br, 2 H, CH<sub>2</sub> pip), 4.26 (m, 2 H, Bzd H-2 or H-3), 4.33 (m, 2 H, Bzd H-2 or H-3), 6.51 (dd, 1 H, Bzd H-6, *J* = 8 and 2), 6.63 (dd, 1 H, Bzd H-8, *J* = 8 and 2), 6.79 (t, 1 H, Bzd H-7, *J* = 8), 7.43 (cluster, 5 H, arom H).

**Biochemistry. Receptor Binding Assay.** The radioligand binding studies were performed on rat frontal cortex using [<sup>3</sup>H]-2-(di-*n*-propylamino)-8-hydroxytetralin as radioligand as described.<sup>13</sup> All *K*<sub>i</sub> ± SEM (nm) values are based on three to six assays, each using four to six concentrations in triplicate.

**Acknowledgment.** The authors wish to thank M. ter Horst-van Amstel for her secretarial assistance.

## References

- Peroutka, S. J. 5-Hydroxytryptamine Receptor Subtypes. *Annu. Rev. Neurosci.* **1988**, *11*, 45–60.

- (2) Frazer, A.; Maayani, S.; Wolfe, B. B. Subtypes of Receptors for Serotonin. *Annu. Rev. Pharmacol. Toxicol.* **1990**, *30*, 307–348.
- (3) Zifa, E.; Fillion, G. 5-Hydroxytryptamine Receptors. *Pharmacol. Rev.* **1992**, *44* (3), 401–458.
- (4) Romero, A. G.; McCall, R. B. Advances in Central Serotonergic. *Annu. Rep. Med. Chem.* **1992**, *270*, 21–30.
- (5) Fuller, R. W.; Robertson, D. W. Progress in Antidepressant Drugs. *Annu. Rep. Med. Chem.* **1991**, *26*, 23–32.
- (6) Glennon, R. A. Concepts for the Design of 5-HT<sub>1A</sub> Serotonin Agonists and Antagonists. *Drug Dev. Res.* **1992**, *26*, 251–274.
- (7) Nelson, D. L. Structure-Activity Relationships at 5-HT<sub>1A</sub> Receptors: Binding Profiles and Intrinsic Activity. *Pharmacol. Biochem. Behav.* **1991**, *40*, 1041–1051.
- (8) Barrett, J. E.; Vanover, K. E. 5-HT Receptors as Targets for the Development of Novel Anxiolytic Drugs: Models, Mechanisms and Future Directions. *Psychopharmacology* **1993**, *112*, 1–12.
- (9) Hamon, M.; Gozlan, H. Central Serotonin Receptors. *Med. Sci.* **1993**, *9*, 21–30.
- (10) Handley, S. L.; McBlane, J. W. 5-HT Drugs and Animal Models of Anxiety. *Psychopharmacology* **1993**, *112*, 13–49.
- (11) van Steen, B. J.; van Wijngaarden, I.; Tulp, M. Th. M.; Soudijn, W. Structure-Affinity Relationship Studies on 5-HT<sub>1A</sub> Receptor Ligands. 1. Heterobicyclic Phenylpiperazines with N<sub>4</sub>-Alkyl Substituents. *J. Med. Chem.* **1993**, *36*, 2751–2760.
- (12) van Wijngaarden, I.; Kruse, C. G.; van der Heyden, J. A. M.; Tulp, M. Th. M. 2-Phenylpyrroles as Conformationally Restricted Benzamide Analogues. A New Class of Potential Antipsychotics. 2. *J. Med. Chem.* **1988**, *31*, 1934–1940.
- (13) Gozlan, H.; El Mestikawy, S.; Pichet, L.; Glowinski, J.; Hamon, M. Identification of Presynaptic Serotonin Autoreceptors Using a New Ligand: [<sup>3</sup>H]-PAT. *Nature* **1983**, *305*, 140–142.
- (14) Normal *t*-test; *p* < 0.05.
- (15) SYBYL Molecular Modelling, version 6.0, Tripos Associates, Inc., St. Louis, MO, running on Silicon Graphics computers (IRIS 4D/320 and IRIS Indigo ELAN 4000).
- (16) Carroll, F. I.; Gao, Y. G.; Rahman, M. A.; Abraham, P.; Parham, K.; Lewin, A. H.; et al. Synthesis, ligand binding, QSAR, and CoMFA study of 3 beta-(p-substituted phenyl)tropane-2 beta-carboxylic acid methyl esters. *J. Med. Chem.* **1991**, *34*, 2719–2725.
- (17) Clark, M.; Cramer, R. D. The Probability of Chance Correlation using Partial Least Squares (PLS). *Quant. Struct.-Act. Relat.* **1993**, *12*, 137–145.
- (18) Wakeling, I. N.; Morris, J. A. A Test of Significance for Partial Least Squares Regression. *J. Chemom.* **1993**, *7*, 291–304.
- (19) Topliss, J. G.; Edwards, R. P. Chance Factors in Studies of Quantitative Structure-Activity Relationships. *J. Med. Chem.* **1979**, *22*, 1238–1244.
- (20) The QSAR module of SYBYL uses tables to store molecules and their properties. For QSAR studies, these tables are organized so that each horizontal row corresponds to a molecule. The corresponding columns are filled with the molecular properties, e.g., binding affinity and log *P*, etc. CoMFA uses the steric (Lennard Jones) and electrostatic field properties and places these descriptors in a large number of columns (CoMFA columns). Partial least squares can then be used to correlate the independent variables (field properties) with the dependent column (affinity).
- (21) Agarwal, A.; Taylor, E. W. 3D QSAR for Intrinsic Activity of 5-HT<sub>1A</sub> Receptor Ligands by the Method of Comparative Molecular Field Analysis. *J. Comput. Chem.* **1993**, *14* (2), 237–245.
- (22) Langlois, M.; Bremont, B.; Rousselle, D.; Gaudy, F. Structural Analysis by the Comparative Molecular Field Analysis Method of the Affinity of beta-Adrenoreceptor Blocking Agents for 5-HT<sub>1A</sub> and 5-HT<sub>1B</sub> Receptors. *Eur. J. Pharmacol.* **1993**, *244*, 77–87.
- (23) Rusinko, A., III; Skell, J. M.; Balducci, R.; McGarity, C. M.; Pearlman, R. S. The University of Texas at Austin and Tripos Associates, St. Louis, MO, 1988.
- (24) MOPAC 6.0 available from Quantum Chemistry Program Exchange.
- (25) Cramer, R. D., III; Bunce, J. D.; Patterson, D. E. Validation, Bootstrapping and Partial Least Squares Compared with Multiple Regression in Conventional QSAR studies. *Quant. Struct.-Act. Relat.* **1988**, *7*, 18–25.
- (26) Hartog, J.; Olivier, B.; van Wijngaarden, I. Japanese Patent Application JP 61,152,655, 1986.
- (27) Egger, J. F.; Melvin, L. S.; Johnson, M. R. European Patent Application EP 90526, 1983.
- (28) Cramer, R. D.; Patterson, D. E.; Brunce, J. D. Comparative Molecular Field Analysis (CoMFA). 1. Effect of Shape on Binding Studies of Steroids to Carrier Proteins. *J. Am. Chem. Soc.* **1988**, *110*, 5959–5967.
- (29) Helland, I. S. Partial Least Squares Regression and Statistical Models. *Scand. J. Statist.* **1990**, *17*, 191–193.
- (30) Hartog, J.; Wouters, W.; van Wijngaarden, I. European Patent Application EP 138280.
- (31) Besides the calculations using all compounds (*n* = 43), we have also run CoMFA with the derivatives of **3** and **4** separately (*n* = 21 and 22, respectively). Similar trends were found in comparison to the combined **3** + **4** series, although the *r*<sup>2</sup><sub>cv</sub> values found for the derivatives of **4** were lower due to a lesser structural differentiation (more alkyl than aralkyl derivatives).